Pathogenic, but not non-pathogenic, *Rickettsia* manipulate inflammasome-dependent IL-1 responses to facilitate their replication and host dissemination.

Author information

Oliver H. Voss[1,*]

Jennifer Cobb[1]

Natalia Rivera Díaz[2]

Rigoberto Sanchez[2]

Louis DeTolla[2]

M. Sayeedur Rahman[1]

Abdu F. Azad[1,*]

[1]Department of Microbiology and Immunology, University of Maryland School of Medicine, Baltimore, MD 21201, USA

[2]Department of Pathology, Comparative Medicine (Infectious Diseases), and Epidemiology and Public Health, University of Maryland School of Medicine, Baltimore, MD 21201, USA

*Correspondence: ovoss@som.umaryland.edu (O.H.V.), aazad@som.umaryland.edu (A.F.A.)

ORCIDs:

Oliver H. Voss: 0000-0002-1436-2809

M. Sayeedur Rahman: 0000-0002-9216-9270

Abdu F. Azad: 0000-0003-1535-6395

Rigoberto Sanchez: 0000-0002-1355-3531

Classification: Biological Sciences: Microbiology

Keywords: *R. typhi*, *R. rickettsii (Sheila Smith)*, *R. montanensis*, IL-1α, IL-1β, Caspase-1, Caspase-11, macrophages, inflammasomes, bacterial host dissemination.

Author Contributions

O.H.V., M.S.R., and A.F.A. planned the research, analyzed, and interpreted the data; O.H.V., J.C., N.R.D., and M.S.R. performed the experiments; A.F.A., O.H.V., L.D., and R.S. contributed to the overall project administration and supervision; O.H.V., M.S.R., and A.F.A. wrote the manuscript; and all authors participated in editing the manuscript.

Abstract

Rickettsia species (spp.) are strict obligate intracellular bacteria, symbiotic in their arthropod vector, and some being pathogenic in their mammalian host, including humans. One critical feature of these stealthy group of pathogens is their ability to manipulate hostile cytosolic environments to their benefits. Although our understanding of *Rickettsia* cell biology and pathogenesis are evolving, the mechanisms of host innate immune defense evasion by pathogenic *Rickettsia* spp. remains to be elucidated. Here, we showed that disease severity in wild-type (WT) C57BL/6J mice infected with *R. typhi*- (etiologic agent of murine *typhus*) and *R. rickettsii* (etiologic agent of Rocky Mountain

Spotted Fever), but not with non-pathogenic *R. montanensis*, correlated with levels of bacterial burden as detected in the spleens, as well as the serum concentrations of pro-inflammatory cytokine IL-1α and to a lesser extent IL-1β. Antibody-mediated neutralization of IL-1α confirmed a key role in controlling mortality rates and bacterial burdens of rickettsiae-infected WT mice. As macrophages are a primary source of both IL-1α and IL-1β cytokines, we determined the mechanism of the anti-rickettsial activities using bone-marrow-derived macrophages. We found that pathogenic *R. typhi* and *R. rickettsii*, but not non-pathogenic *R. montanensis*, induced autophagy, and avoided autophagolysosomal destruction, while simultaneously eluded pro-IL-1α induction and benefited from the dampening of IL-1α secretion, via Caspase-11-Gsdmd-dependent mechanism, to facilitate intracytosolic replication. Adoptative transfer experiments identified that IL-1α secretion by macrophages was critical for controlling rickettsiosis in WT mice. In sum, we identified a previously unappreciated pathway by which pathogenic, unlike non-pathogenic, rickettsiae preferentially target the Caspase-11-Gsdmd-IL-1α signaling axis in macrophages, possibly via an autophagy-dependent mechanism, to support their replication and dissemination within the host.

Significance Statement

Currently, no vaccines are available to prevent rickettsioses, and tick- and flea-borne rickettsial infections in humans are on the rise globally. In fact, the insufficient understanding of how pathogenic *Rickettsia* species circumvent host immune defense mechanisms has significantly hindered the development of more effective therapeutics. Here, we identified a previously unappreciated role for the Caspase-11-Gsdmd-IL-1α

70 signaling axis, to limiting the survival and dissemination of pathogenic *R. rickettsia* and
71 *R. typhi* species in macrophages and wild-type C57BL/6J mice. Adoptative transfer
72 studies further identified IL-1α-secreting macrophages as critical mediators in controlling
73 rickettsial infection in WT mice. Collectively, these findings provide insight into the
74 potential mechanism of how pathogenic, but not non-pathogenic *Rickettsia* spp., become
75 ubiquitinated, induce autophagy and benefit from the dampening of the Caspase-11-
76 Gsdmd-mediated release of IL-1α to support host colonization.
77
78 **Introduction**

79 Invasive cytosolic bacteria, including *Listeria*, *Shigella*, *Burkholderia*, *Francisella*,
80 *Orientia*, and *Rickettsia* species (spp.) have developed strategies to induce their own
81 uptake by phagocytosis and to circumvent host innate immune defenses for their
82 intracellular survival (Personnic et al., 2016; Ray et al., 2009). Human infection with
83 *Rickettsia* spp. occurs via infected hematophagous arthropods such as ticks, fleas, and
84 human body lice (Sahni et al., 2018) either through the bite or deposited infected feces
85 into skin and mucosal surfaces. Upon entry, *Rickettsia* spp. encounter tissue-resident
86 immune cells, like macrophages (MΦ). Activated MΦ play a crucial role in either
87 terminating an infection at an early stage, which commonly is the fate of non-pathogenic
88 *Rickettsia* spp., or succumbing to bacterial replication and pathogen colonization as well
89 as host dissemination to distant organs (Sahni et al., 2018). After internalization into host
90 cells, *Rickettsia* spp. escape from phagosomes and subvert host cytosolic defense
91 mechanisms (*i.e.*, autophagy and inflammasomes) to establish an intracytosolic
92 replication niche. Recently, we reported that pathogenic *Rickettsia* spp. secret effectors
93 to promote host colonization by modulating endoplasmic reticulum structures or by

94 hijacking the autophagic defense pathway (Lehman et al., 2018; Rahman et al., 2010,
95 2013; Rennoll-Bankert et al., 2015, 2016; Voss et al., 2020). Subversion of autolysosomal
96 destruction to colonize the host cytosol exposes *Rickettsia* spp. to another cytosolic host
97 sensor-regulated defense mechanism, the inflammasomes (Ray et al., 2009; Sun et al.,
98 2017). Inflammasomes are immune signaling complexes categorized into canonical
99 [Caspase (Casp)-1] and non-canonical [murine Casp-11 or human Casp-4/5]
100 inflammasomes. The inflammasome complex assembly involves the adaptor protein ASC
101 and upstream sensors including NLRP1, NLRP3, NLRC4, AIM2, and pyrin, and is
102 activated by both exogenous pathogen-associated molecular pattern molecules (PAMPs)
103 and endogenous damage-associated molecular pattern molecules (DAMPs). Initiation of
104 the canonical inflammasome results in the activation of Casp-1. Active Casp-1 leads to
105 the maturation of proinflammatory cytokines IL-1β and IL-18 and the activation of
106 gasdermin D (Gsdmd), the executor of pyroptosis (Place and Kanneganti, 2018; Xue et
107 al., 2019). Although IL-1β is released by both canonical and non-canonical inflammasome
108 pathways, IL-1α is induced preferentially by the non-canonical inflammasome pathway
109 (Malik and Kanneganti, 2018; Tapia et al., 2019; Wiggins et al., 2019). IL-1α is expressed
110 by a wide range of hematopoietic and non-hematopoietic cell types, whereas IL-1β is
111 primarily produced by myeloid cells (Malik and Kanneganti, 2018). Importantly, although
112 IL-1α and IL-1β signal through the same receptor, IL-1R, these two cytokines are not
113 completely functionally redundant (Malik and Kanneganti, 2018). Given the importance
114 for both canonical and non-canonical inflammasome-mediated IL-1 signaling in limiting
115 pathogen dissemination, many bacteria have evolved strategies to block their activation
116 (Krakauer, 2019; Mitchell and Isberg, 2017; Seveau et al., 2018; Storek and Monack,

117 2015; Vladimer et al., 2013; Zheng et al., 2020). In fact, various pathogenic intracellular
118 bacteria utilize their own effector repertoire to evade these pathways to successfully
119 replicate and disseminate in their host cells (Sun et al., 2017; Takahama et al., 2018).
120 In the case of *Rickettsia*, our understanding of the role of inflammasomes in controlling
121 host colonization is only now emerging (Bechelli et al., 2018; Burke et al., 2020; Engström
122 et al., 2019; Smalley et al., 2016). Specifically, how pathogenic *Rickettsia* spp. manipulate
123 immune defenses to replicate within the host cytosol not only relies almost exclusively on
124 data from tick-transmitted rickettsiae [*e.g.*, members of spotted fever group (SFG) or
125 transition group (TRG)], but also shows that these pathogens likely employ species-
126 specific strategies to evade host cytosolic defense mechanisms. For instance, *R.*
127 *australis*, a pathogenic TRG member, benefited from ATG5-mediated autophagy
128 induction and suppression of inflammasome-dependent IL-1β production to colonize both
129 BMDMΦ (Bechelli et al., 2018) and mice (Rumfield et al., 2020). In contrast, *R. parkeri*, a
130 mildly pathogenic member of SFG (see Figure 1A), utilizes its surface cell antigen Sca5
131 (OmpB) for protection against autophagic recognition, and consequently benefits from
132 inflammasome-mediated host cell death that antagonizes the action of Type I IFN in
133 BMDMΦ and mice (Burke et al., 2020; Engström et al., 2019). In contrast, our recent
134 report on the flea-transmitted *R. typhi* [pathogenic member of typhus group (TG)], showed
135 that *R. typhi* is ubiquitinated upon host entry and escapes autolysosomal fusion to
136 establish an intracytosolic niche in non-phagocytic cells (Voss et al., 2020). These
137 unexpected findings on how SFG, TRG, and TG *Rickettsia* differentially promote their
138 host dissemination prompted us to explore the underlying mechanism(s) by which
139 pathogenic, but not non-pathogenic, *Rickettsia* spp. manipulate immune defenses to

140 establish a replication niche in phagocytic cells, like MΦ. Specifically, we sought to test
141 the hypothesis that pathogenic, but not non-pathogenic, *Rickettsia* spp. induce
142 autophagy, but evade autophagolysosomal destruction, to dampen inflammasome-
143 mediated IL-1 responses thereby promoting their intracytosolic replication as well as host
144 dissemination.
145
146 **Results**
147 ***In vivo* models of rickettsiosis**.
148 At present, more than 30 *Rickettsia* spp. have been described globally, but less than
149 a dozen is known to cause disease in humans, with some being notoriously pathogenic
150 and associated with high morbidity and mortality, while others exert limited or no
151 pathogenicity (Figure 1A). We sought to test our hypothesis that pathogenic, but not non-
152 pathogenic, *Rickettsia* spp. manipulate immune responses in host defense cells, like MΦ,
153 to replicate and disseminate. We simultaneously evaluated the cytosolic host defense
154 responses between pathogenic [*R. rickettsii (Sheila Smith, SS)* and *R. typhi* (Wilmington)
155 and non-pathogenic (*R. montanensis*) strains *in vivo*. We first established a mouse model
156 of mild (~LD_{25}) or more severe (~LD_{50}) rickettsiosis in C57BL/6J WT mice. For both *R.*
157 *rickettsii* and *R. typhi* LD_{25} or LD_{50} were achieved with doses of 10^5 or 10^6 PFU,
158 respectively (Figures 1B-C), however, *R. montanensis*-infected mice showed no signs of
159 lethality at either 10^5 or 10^6 PFU (Figure 1D), Bacterial burden in spleens from infected
160 C57BL/6J WT mice (only dose of 10^6 PFU is shown) confirmed successful infection with
161 all three *Rickettsia* spp. at day 3 post-infection, while *R. typhi*- and *R. rickettsii*-infected
162 WT mice displayed significantly higher bacterial burden in the spleens as compared to

163 splenic tissues from *R. montanensis*-infected mice at day 7 (Figure 1E). This correlated
164 with the observed differences in the spleen sizes and weights of the infected animals
165 (Figure S1), suggesting more efficient clearance of *R. montanensis* compared to the
166 pathogenic strains. Given the earlier findings from other laboratories and ours (Bechelli
167 et al., 2018; Burke et al., 2020; Engström et al., 2019; Papp et al., 2016; Rumfield et al.,
168 2020; Smalley et al., 2016; Voss et al., 2020), we hypothesized that the observed
169 dissimilarities in pathogenicity among *Rickettsia* spp. is likely linked to differences in host
170 defense responses. Recent findings further suggest that the intracytosolic survival of
171 different *Rickettsia* spp. is either supported or suppressed by immune defense responses
172 (*e.g.*, IFN-I, TNF-α, or IL-1β) (Bechelli et al., 2018; Burke et al., 2020; Engström et al.,
173 2019; Papp et al., 2016; Rumfield et al., 2020; Smalley et al., 2016), leaving the precise
174 mechanism to be determined. Therefore, we first sought to evaluate the canonical and
175 non-canonical inflammasome responses at the level of IL-1β and IL-1α cytokine secretion
176 in the sera of *R. typhi*-, *R. rickettsii*-, and *R. montanensis*-infected animals. The increase
177 in mortality and elevated bacterial burden correlated with reduced serum levels of both
178 IL-1β and IL-1α cytokines (Figures 1F-G), suggesting that dampening of both canonical
179 and non-canonical inflammasome-dependent signaling responses is a potential
180 mechanism for lethality and dissemination of pathogenic *Rickettsia* spp.
181
182 **Anti-rickettsial activity of IL-1α is involved in restricting *Rickettsia* infection.**
183 To characterize further the role of IL-1α and IL-1β cytokines in restricting non-
184 pathogenic and pathogenic *Rickettsia* spp. *in vivo*, IL-1α or IL-1β function was neutralized
185 via tail vein (*i.v.*) injection, with anti(α)-IL-1α, αIL-1β, or αIgG-isotype control antibodies

186 (Abs) into C57BL/6J WT mice in our established model of mild rickettsiosis (LD_{25}; ~10^5
187 PFU, Figures 1B-D). Neutralization of IL-1α, and to a much lesser extent IL-1β, was
188 associated with a significant increase in the mortality of *R. typhi*-, *R. rickettsii*-, and *R.*
189 *montanensis*-infected mice (Figures 2A-C) and resulted in the development of
190 splenomegaly (Figure S2), which correlated with an increase in bacterial loads in the
191 spleen (Figure 2D). The efficiency of Ab-mediated blocking was confirmed by measuring
192 the levels of IL-1β and IL-1α cytokine in the sera of the rickettsiae-infected mice (Figures
193 2E-F). Next, we sought to determine the effect of administering recombinant (r)IL-1α or
194 rIL-1β proteins on *Rickettsia* dissemination *in vivo*. Accordingly, we administered (*i.v.*)
195 endotoxin-free rIL-1α and rIL-1β proteins following infection with *R. typhi*, *R. rickettsii*, and
196 *R. montanensis*. Pretreatment of mice with rIL-1α, and to a lesser extent rIL-1β, protected
197 C57BL/6J WT mice from pathogenic *Rickettsia*-induced lethality (Figures S3A-C),
198 significantly reduced development of splenomegaly, and caused a decrease in the
199 bacterial burden in the spleens of infected animals (Figures S3D-F). Moreover, the
200 observed phenotypes correlated with the measured IL-1α and IL-1β serum concentrations
201 (Figures S3G-H). Collectively, these findings suggest that IL-1α, and to a lesser extent,
202 IL-1β, are involved in restricting the replication and dissemination of non-pathogenic and
203 pathogenic *Rickettsia* spp.
204

205 **Pathogenic *Rickettsia* species dampen pro-IL-1α induction and Caspase-11-**
206 **dependent IL-1α secretion to establish a replication niche in macrophages.**

207 As MΦ are one of the cell types first encountered during infection by *Rickettsia* spp.
208 and are considered to play a crucial role in either terminating the infection early at the

209 skin site or allow pathogen colonization and subsequent dissemination within the infected
210 host (Sahni et al., 2018), we tested the hypothesis that pathogenic, but not non-
211 pathogenic, rickettsiae dampen MΦ immune responses. In this effort, we infected
212 BMDMΦ derived from WT mice with pathogenic *R. typhi* and *R. rickettsii* or non-
213 pathogenic *R. montanensis* and assessed first the canonical and non-canonical
214 inflammasome-dependent IL-1 responses. Our assays revealed that *R. typhi*- or *R.*
215 *rickettsii*-infected BMDMΦ WT produced lower levels of IL-1β and IL-1α, and showed
216 significantly lesser induction of host cell death, as compared to *R. montanensis*-infected
217 BMDMΦ WT (Figures 3A-I, black squares). In addition, the reduced levels of IL-1
218 responses and host cell death correlated with an elevated bacterial burden (Figure 3J,
219 black squares). Importantly, and in agreement with our *in vivo* data (Figure 1E), *R. typhi*-
220 or *R. rickettsii*-infected BMDMΦ WT displayed, over the course of infection, a higher
221 bacterial burden than *R. montanensis*-infected BMDMΦ WT (Figure 3J, 2 *vs.* 24 h black
222 squares), suggesting more efficient clearance of *R. montanensis* compared to the
223 pathogenic strains (Figures 3J and 1E). To determine the importance of IL-1α and IL-1β
224 in restricting the replication of pathogenic and non-pathogenic *Rickettsia* spp. in MΦ, we
225 infected BMDMΦ derived from WT, IL-1α-, or IL-1β-deficient mice with all three *Rickettsia*
226 spp. and assessed the cytokine levels of IL-1β and IL-1α in cultured supernatants as well
227 as bacterial burdens. As anticipated, infection of IL-1$\beta^{-/-}$ or IL-1$\alpha^{-/-}$ BMDMΦ with *Rickettsia*
228 spp. did not result in the secretion of either IL-1β or IL-1α, respectively, when compared
229 to infected WT BMDMΦ (Figures S4A-F). Moreover, infections with *R. montanensis*
230 resulted in overall higher IL-1 responses and lower bacterial burden when compared to
231 infections performed with *R. typhi* or *R. rickettsii* in WT, IL-1$\beta^{-/-}$, or IL-1$\alpha^{-/-}$ BMDMΦ

232 (Figures S4A-G). Of note, the bacterial burden of all three *Rickettsia* spp. in infected IL-
233 1α$^{-/-}$ BMDMΦ was higher than the levels detected in IL-1β$^{-/-}$ or WT BMDMΦ (Figures
234 S4G), suggesting that IL-1α and to significantly lesser extent IL-1β, plays a role in
235 restricting rickettsiae survival. As our findings suggest that pathogenic, but not non-
236 pathogenic, *Rickettsia* spp. can dampen IL-1α and IL-1β secretion, we explored the
237 mechanism of IL-1 signaling responses in greater detail. First, we assessed the protein
238 expression levels of pro-IL-1β and -IL-1α in WT BMDMΦ upon *Rickettsia* infection and
239 showed that pro-IL-1β levels were induced by all three *Rickettsia* spp. to similar levels
240 (~5-fold) when compared to uninfected WT BMDMΦ (Figure S4H). Intriguingly, only *R.*
241 *montanensis*-infected WT BMDMΦ produced significantly higher levels of pro-IL-1α, as
242 compared to *R. typhi*- or *R. rickettsii*-infected MΦ (Figure S4H). As IL-1 signaling
243 responses require canonical and non-canonical inflammasome pathways, which in turn
244 involves the proteolytic processing of both cytokines by activated Caspase (Casp)-1
245 (canonical) and Casp-11 (non-canonical) respectively, we assessed the potential role of
246 Casp-1 and Casp-11 in regulating replication of non-pathogenic *vs*. pathogenic *Rickettsia*
247 in BMDMΦ. In this effort, BMDMΦ derived from WT, Casp-1$^{-/-}$, Casp-11$^{-/-}$, and Casp-1/11^{-}
248 $^{/-}$ mice were infected with *R. typhi*, *R. rickettsii*, and *R. montanensis* and the levels of IL-
249 1β and IL-1α, as well as bacterial burdens, were evaluated over the course of infection.
250 Our assays revealed that Casp-11 was involved in the secretion of cleaved IL-1α, and to
251 a lesser extent cleaved IL-1β, upon infection of BMDMΦ with non-pathogenic and
252 pathogenic *Rickettsia* spp. (Figures 3A-B, D-E, and G-H; Casp-11$^{-/-}$; Casp-1/11$^{-/-}$). In
253 addition, Casp-11 deficiency resulted in a significant decrease in host cell death (Figures
254 3C, F, and I). Casp-1 deficiency (Casp-1$^{-/-}$) caused a significant decrease in IL-1β

255 production [Figures 3A, D, and G (green lines)], while IL-1α secretion as well as the level
256 of cell death remained unaffected during infection with all three *Rickettsia* spp. [Figures
257 3B-C, E-F, and H-I (green lines, symbols)]. Analysis of bacterial burdens further revealed
258 a prominent role for Casp-11, but not Casp-1, in restricting the replication of both
259 pathogenic and non-pathogenic *Rickettsia* spp. (Figure 3J; WT (square symbols); Casp-
260 $1^{-/-}$ (sphere symbols); Casp-$11^{-/-}$ (triangles symbols); Casp-1/$11^{-/-}$ (diamond symbols)]. As
261 our findings indicate that infections with *R. typhi*- and *R. rickettsii* resulted in a significant
262 reduction of IL-1α secretion, likely via Casp-11-dependent mechanism, we assessed the
263 expression and activation status of Casp-1 and Casp-11 via Western blot analyses. As
264 anticipated, *R. montanensis* infection resulted in a robust activation of Casp-1, as
265 indicative of the detection of the Casp-1-p20 fragment (Figure 3K). In contrast, infection
266 with *R. typhi* and *R. rickettsii* spp. resulted in a lower activation of Casp-1 (~5-fold) (Figure
267 3K). Intriguingly, only infection with *R. montanensis* resulted in a robust induction of Casp-
268 11 (~8 fold) as compared to infection data using both pathogenic *Rickettsia* spp. (Figure
269 3K). As IL-1 cytokine secretion dependents on Gsdmd, the pore-forming executor of
270 pyroptosis (Batista et al., 2020; Kanneganti et al., 2018; Liu et al., 2016; Tsuchiya et al.,
271 2021), we assessed the proteolytic processing of Gsdmd and showed that only *R.*
272 *montanensis* infection resulted in a robust cleavage of Gsdmd (~8 fold), as indicative by
273 the detection of the Gsdmd-p30 fragment (Figure 3K). In support of our findings, we
274 showed that infection of $Gsdmd^{-/-}$ BMDMΦ with non-pathogenic and pathogenic
275 *Rickettsia* spp. released significantly lower levels of IL-1β and IL-1α, as compared to WT
276 BMDMΦ (Figures S5A-B). Furthermore, analysis of bacterial burdens provided additional
277 evidence that Gsdmd plays a role in restricting the replication of *R. typhi*, *R. rickettsii*, and

278 *R. montanensis*, (Figure S5C). These findings suggest that pathogenic, unlike non-
279 pathogenic, *Rickettsia* spp. differentially modulate pro-IL-1 induction and dampen IL-1
280 cytokine secretion, likely via a Casp-11-Gsdmd-dependent mechanism, to support
281 replication in MΦ.
282
283 **Ubiquitination and autophagy induction contribute to the survival of pathogenic**
284 ***Rickettsia* species in macrophages.**
285 Preceding findings suggest that intracellular pathogens, like rickettsiae, not only
286 encounter inflammasome-dependent defense mechanisms but are also confronted by
287 another cytosolic defense pathway, autophagy (Bechelli et al., 2018; Smalley et al.,
288 2016). Both responses not only are key to mount the appropriate host defense responses
289 (Krakauer, 2019; Seveau et al., 2018) but are also functionally interconnected. In fact,
290 recent reports indicated that autophagy acts on intracellular microbes upstream of the
291 inflammasome and thereby functions as a negative regulator by degrading inflammasome
292 components (Krakauer, 2019; Seveau et al., 2018; Sun et al., 2017; Takahama et al.,
293 2018). In the case of rickettsiae, however, the role of autophagy in regulating
294 inflammasome responses to facilitate their host colonization remains inconclusive. For
295 instance, *R. australis*, a pathogenic TRG member, benefited from ATG5-dependent
296 autophagy induction and suppression of inflammasome-dependent IL-1β production to
297 colonize MΦ (Bechelli et al., 2018; Smalley et al., 2016). In contrast, *R. parkeri*, a mildly
298 pathogenic member of SFG, demonstrated that its surface protein OmpB is critical for
299 protecting against autophagic recognition, while evasion of autophagy was critical for
300 invasion of BMDMΦ and WT mice by *R. parkeri* (Burke et al., 2020; Engström et al.,

301 2019). Intriguingly, our recent report on *R. typhi* showed that *R. typhi* is ubiquitinated upon
302 host entry, induces autophagy, but escapes autophagolysosomal maturation for
303 intracellular colonization in non-phagocytic cells (Voss et al., 2020). Given these reports
304 by others and our recent findings, we hypothesized that pathogenic, but not non-
305 pathogenic, *Rickettsia* spp. induce autophagy and down-regulate IL-1β and IL-1α
306 cytokine responses to establish a replication niche in MΦ. To test this hypothesis, we first
307 evaluated the ubiquitination status of *R. typhi*, *R. rickettsii*, or *R. montanensis*, during
308 invasion of BMDMΦ derived from WT mice. Our data showed, similar to infection studies
309 using *R. australis* (Bechelli et al., 2018), both pathogenic *R. rickettsii*, and *R. typhi* strains
310 were ubiquitinated upon entry into WT BMDMΦ (Figures S6A-B). In contrast, but similar
311 to infection studies using *R. parkeri*, non-pathogenic *R. montanensis* was not
312 ubiquitinated during infection of WT BMDMΦ (Figures S6A-B), suggesting that *R.*
313 *montanensis* is likely destroyed by phagolysosomal fusion before escaping into cytosol
314 of MΦ. Furthermore, we evaluated the status of autophagy markers p62 (SQSTM1) and
315 autophagic vesicle formation marker LC3B (Klionsky et al., 2016) during infection of WT
316 BMDMΦ by Western blot analyses and showed that, unlike *R. montanensis*, infection with
317 both pathogenic *Rickettsia* spp. increased autophagic flux, as evidenced by an enhanced
318 induction of LC3B and the simultaneously down-regulation of p62 expression (Figure
319 S6C). To further confirm the observation that pathogenic, but not non-pathogenic,
320 *Rickettsia* spp. could modulate autophagy flux, we evaluated the status of LC3B
321 during infection of ATG5$^{fl/fl}$ or ATG5$^{fl/fl}$-LysM-Cre BMDMΦ by immunofluorescence assay
322 (IFA). We showed that, unlike *R. montanensis*, *R. typhi*, and *R. rickettsii* colocalized with
323 LC3B upon entry of ATG5$^{fl/fl}$ MΦ, but not in ATG5$^{fl/fl}$-LysM-Cre MΦ (Figures 4A-D). Given

324 that *R. typhi* was shown to be capable of avoiding autolysosomal destruction in non-
325 phagocytic cells (Voss et al., 2020), we evaluated the colocalization pattern of rickettsiae
326 with the lysosomal marker Lamp2 and showed that, unlike non-pathogenic *R.*
327 *montanensis*, both *R. typhi*, and *R. rickettsii* spp., did not colocalize with Lamp2 in ATG5$^{fl/fl}$
328 MΦ (Figures 4A-D), while all three rickettsiae strains colocalized with Lamp2 in ATG5$^{fl/fl}$-
329 LysM-Cre MΦ (Figures 4A-D), suggesting that pathogenic *Rickettsia* spp. abate
330 autophagosomal maturation. Given these data, we sought to study further the autophagy
331 induction by *Rickettsia* spp. utilizing an inhibitor of autophagy, 3-methyladenine (3-MA).
332 Similar to our infection studies using ATG5-deficient MΦ, treatment of WT BMDMΦ with
333 3-MA significantly decreased the number of LC3B^{+}-bacteria (Figures S7A-G).
334 Importantly, 3-MA treatment increased the number of Lamp2^{+}-pathogenic rickettsiae
335 (Figures S7A-G), providing further support to our hypothesis that pathogenic *Rickettsia*
336 spp. rely on the initiation of autophagy and escape from autophagolysosomal destruction
337 to establish a replication niche. To test if autophagy was involved in the dampening of the
338 inflammasome-dependent IL-1 cytokine responses, we evaluated the IL-1β and IL-1α
339 cytokine levels in cultured supernatants of rickettsiae-infected ATG5$^{fl/fl}$ and ATG5$^{fl/fl}$-LysM-
340 Cre BMDMΦ. Lack of autophagy was associated with an increase in the secretion of IL-
341 1β or IL-1α upon infection with non-pathogenic as well as pathogenic *Rickettsia* spp.
342 (Figure 4E). Collectively, our data are in agreement with previous reports (Bechelli et al.,
343 2018; Voss et al., 2020), indicating that, unlike non-pathogenic *R. montanensis* spp., both
344 pathogenic *R. typhi*, and *R. rickettsii* spp., induce autophagy but avoid
345 autophagolysosomal destruction, as well as dampen anti-rickettsial inflammasome-

346 dependent IL-1 cytokine responses during establishment of an intracytosolic replication
347 niche in MΦ.
348
349 **Secretion of IL-1α by macrophages is crucial in restricting the survival and**
350 **dissemination of pathogenic and non-pathogenic *Rickettsia* species.** To examine
351 whether secretion of IL-1 by MΦ limits the replication of *Rickettsia* spp. *in vivo*, we first
352 injected (*i.v.*) WT mice with PBS- or dichloromethylene biphosphate (Cl_2MBP)-liposomes
353 to deplete endogenous macrophages as described previously (Voss et al., 2016). Next,
354 PBS- or Cl_2MBP-liposomes treated WT mice were injected (*i.v.*) with BMDMΦ isolated
355 from WT, IL-1β$^{-/-}$, or IL-1α$^{-/-}$ mice prior to infection with *R. typhi*, *R. rickettsii*, or *R.*
356 *montanensis*. Strikingly, adoptive transfer of IL-1α$^{-/-}$ BMDMΦ, but not IL-1β$^{-/-}$, or WT MΦ,
357 significantly increased the mortality of Cl_2MBP- but not PBS-treated WT mice injected
358 with all three *Rickettsia* spp., reaching levels similar to the survival percentages observed
359 in IL-1α Ab-neutralization studies (Figures 5A-D, Figures S8A-D and Figure 2). Moreover,
360 transfer of IL-1α$^{-/-}$ BMDMΦ resulted in the development of splenomegaly (Figures S8E-
361 F) and an increase in bacterial burden in the spleens of Cl_2MBP-treated WT mice (Figure
362 5E), which correlated with a decrease in IL-1α serum concentrations without affecting IL-
363 1β serum levels (Figures 5F-G). In contrast, transfer of IL-1β$^{-/-}$ BMDMΦ, had an overall
364 lesser effect on the severity of rickettsiosis, as evidenced by a lower mortality rate, smaller
365 spleen size, and lower bacterial burden in Cl_2MBP-treated WT mice (Figures 5A-D, and
366 Figure S8), which is in agreement with our IL-1β Ab-neutralization data (Figure 2). In
367 addition, transfer of IL-1β$^{-/-}$ BMDMΦ, resulted in a decrease in IL-1β serum concentrations
368 without affecting IL-1α serum levels (Figures 5F-G). In sum, our data presented herein

369 suggest a model by which pathogenic *Rickettsia* spp. become ubiquitinated, induce
370 autophagy, and avoid autophagolysosomal destruction, while elude pro-IL-1α induction
371 and diminish IL-1α secretion, likely by dampening the Casp-11-Gsdmd pathways, to
372 facilitate intracytosolic replication in MΦ and ultimately cause host dissemination (Figure
373 5H).
374
375 **Discussion**
376 Obligate intracytosolic bacterial pathogens, which successfully reside and replicate
377 within the host cytosol, overcome mechanisms of innate immune defense surveillance,
378 including inflammasomes and autophagy. However, in the case of strict obligate
379 intracellular *Rickettsia* spp., the roles for both inflammasome and autophagy to restrict
380 their replication in endothelial cells and immune cells, like MΦ, is only now emerging,
381 although without consistent mechanistical insights (Bechelli et al., 2018; Burke et al.,
382 2020; Engström et al., 2019; Moderzynski et al., 2016; Papp et al., 2016; Rumfield et al.,
383 2020; Smalley et al., 2016). Given these knowledge gaps and our current lack of
384 understanding on how TG *Rickettsia* spp. modulate inflammasome and autophagy
385 pathways to facilitate host dissemination, we established an animal model of rickettsiosis
386 using C57BL/6J WT mice by comparing both mild (~LD_{25}) and more severe disease
387 (~LD_{50}) development for two pathogenic spp., *R. rickettsii*, and *R. typhi*. In fact, data of
388 disease severity correlated with the levels of bacterial burden detected in the mice
389 spleens. We also observed that infections with pathogenic, but not non-pathogenic,
390 *Rickettsia* spp. resulted in a reduced serum response of both pro-inflammatory cytokines,
391 IL-1β and IL-1α, which is likely the result of pathogenic *Rickettsia* spp. to evade canonical

392 and non-canonical inflammasome-dependent defense sensing, of which the former is in
393 agreement with recent studies using *R. australis* (Rumfield et al., 2020). Thus, our data
394 suggests that a dampening of both canonical and non-canonical inflammasome-
395 dependent signaling contributes to the enhanced survival and dissemination of
396 pathogenic *Rickettsia* spp. in our *in vivo* experiments.

397 Our data further suggest that IL-1α, and to significantly lower extent IL-1β, plays a role
398 in limiting rickettsial infection *in vivo*. By testing the putative anti-rickettsial capabilities of
399 these cytokines through employing Ab-neutralization and recombinant protein assays, we
400 showed that IL-1α, and to a much lesser level IL-1β, was able to restrict the replication
401 and dissemination of both non-pathogenic and pathogenic *Rickettsia* spp. *in vivo*. Our
402 current understanding by which *Rickettsia* spp. evade host-induced anti-bacterial
403 activities, and in particular, how cytosolic rickettsiae overcome host immune surveillance
404 in defense cells, like MΦ, is primarily based on inconsistent reports (Bechelli et al., 2018;
405 Burke et al., 2020; Engström et al., 2019; Smalley et al., 2016). Thus, we sought to
406 address the hypothesis that pathogenic *R. typhi*, and *R. rickettsii* spp. but not non-
407 pathogenic *R. montanensis* dampen immune defense responses in order to establish an
408 intracytosolic replication niche in MΦ. In agreement with our *in vivo* infection models, *R.*
409 *montanensis*-infected WT BMDMΦ produced higher levels of IL-1α and IL-1β cytokines
410 and displayed reduced bacterial loads during the course of infection, compared to *R.*
411 *typhi*- or *R. rickettsii*-infected BMDMΦ. These data support the notion that non-
412 pathogenic, but not pathogenic, *Rickettsia* spp. are more efficiently cleared by MΦ, a
413 mechanism that further supports the previously published findings with SFG *Rickettsia*
414 using THP-1 cells, a human macrophage-like cell line (Curto et al., 2016).

415 After internalization by MΦ, intracellular pathogens encounter host innate defense
416 mechanisms, notably autophagy and inflammasome-mediated responses (Krakauer,
417 2019; Seveau et al., 2018). Intriguingly, both pathways are functionally linked, and recent
418 reports suggest a mechanism by which autophagy acts on intracellular microbes
419 upstream of the inflammasome and thereby functions as a negative regulator by
420 degrading inflammasome components (Krakauer, 2019; Seveau et al., 2018; Sun et al.,
421 2017; Takahama et al., 2018). However, the role of autophagy in controlling host
422 colonization of *Rickettsia* spp. remained a matter of debate (Bechelli et al., 2018;
423 Engström et al., 2019). For example, pathogenic *R. australis* benefited from autophagy
424 induction and suppression of inflammasome-dependent IL-1β secretion to colonize
425 BMDMΦ (Bechelli et al., 2018), while mildly pathogenic *R. parkeri* utilization of its surface
426 protein OmpB was critical for its evasion of autophagy and invasion of C57BL/6J BMDMΦ
427 and WT mice (Burke et al., 2020; Engström et al., 2019). Given that OmpB (Sca5) is
428 predicted to be expressed in most if not all *Rickettsia* spp. (Voss and Rahman, 2021),
429 likely implies that the observed OmpB-dependent route of autophagy evasion is a
430 species-specific mechanism employed by *R. parkeri*. This idea is further supported by
431 previously published findings for *R. typhi* (Voss et al., 2020) and *R. australis* (Bechelli et
432 al., 2018), which showed that both pathogenic *Rickettsia* spp. benefited from autophagy
433 to colonize host cells. In an attempt to decipher the mechanism of host-defense evasion,
434 we tested if pathogenic, but not non-pathogenic, *Rickettsia* spp. induce autophagy and
435 down-regulate inflammasome responses to establish a replication niche in MΦ. Our data
436 reveals that, like *R. parkeri*, non-pathogenic *R. montanensis* is not ubiquitinated during
437 infection of MΦ, while both pathogenic *R. typhi*, and *R. rickettsii* are ubiquitinated upon

438 MΦ entry, which is in agreement with reports on pathogenic *R. australis* (Bechelli et al.,
439 2018). In addition, we showed that, unlike *R. montanensis*, *R. typhi*, and *R. rickettsii*
440 colocalized with LC3B, but not with the lysosomal marker Lamp2, after MΦ entry.
441 Importantly, our presented data using the pharmacological inhibitor of autophagy, 3-MA,
442 or ATG5-deficient MΦ further strengthen our hypothesis that pathogenic, but not non-
443 pathogenic, *Rickettsia* spp. induce autophagy but avoid autophagolysosomal destruction
444 and subsequently dampening anti-rickettsial inflammasome-dependent IL-1 cytokine
445 responses to establish an intracytosolic replication niche in MΦ.

446 Of interest, our findings also raised another intriguing question as to why pathogenic
447 *R. typhi*, and *R. rickettsii* spp. seem to possess the ability to actively induce autophagy,
448 while non-pathogenic *R. montanensis* did not. As *Rickettsia*-specific immunodominant
449 outer membrane proteins (*e.g.*, Scas) are predicted to be expressed on either pathogenic
450 or non-pathogenic *Rickettsia* spp. (Voss and Rahman, 2021), one alternative explanation
451 is the presence of an effector repertoire that differs depending on the rickettsial
452 pathogenicity. In fact, we recently reported that pathogenic *R. typhi* induces autophagy
453 upon infection of non-phagocytic cells, while subsequently avoiding autophagosomal
454 destruction, via the secretion of its phosphatidylinositol 3-kinase (PI3K) effector,
455 *Rickettsia* intracellular secreted kinase-1 (Risk1) and phospholipases (e.g., patatin (Pat)-
456 1 and -2) (Voss et al., 2020; Voss and Rahman, 2021). This mechanism of host invasion
457 seems fairly consistent with rickettsial close relatives, such as *Anaplasma*
458 *phagocytophilum* and *Ehrlichia chaffeensis* (Lin et al., 2016; Rikihisa, 2017, 2019;
459 Rikihisa and Lin, 2010), or other intracellular pathogens such as *Shigella* (Campbell-
460 Valois et al., 2015; Ogawa et al., 2005). So, it is tempting to speculate that effectors, like

461 Risk1 and Pat1/2 (either alone or in combination with other currently unknown effectors),
462 could account for the observed phenotypic difference between pathogenic and non-
463 pathogenic *Rickettsia* spp. However, the precise composition of the effector repertoire for
464 each *Rickettsia* spp. is currently a matter of active research, and therefore, the precise
465 mechanism remains to be defined.

466 Given that IL-1 signaling is modulated through inflammasome-dependent Casp-1,
467 Casp-11, and Gsdmd activation, we tested the role of both caspases as well as Gsdmd,
468 and found that non-pathogenic, but not pathogenic, *Rickettsia* spp. ensued Casp-1
469 activation and Casp-11 induction, which ultimately resulted in the proteolytic processing
470 of Gsdmd and release of IL-1α and IL-1β cytokines. Intriguingly, the lack of Casp-11
471 induction by pathogenic, but not non-pathogenic, *Rickettsia* spp. suggest that the
472 membrane-bound LPS of *R. typhi*, and *R. rickettsii* spp. is less immunogenic than that of
473 *R. montanensis*, which is further supported by our recent reports (Guillotte et al., 2018;
474 Guillotte et al., 2021). Our findings further suggest that pathogenic, as compared to non-
475 pathogenic, *Rickettsia* spp., benefit from the dampening of the Casp-11-Gsdmd-IL-1α
476 signaling axis to establish a replication niche in MΦ as evidenced by the increased
477 replication in MΦ from Casp-11$^{-/-}$, Casp-1/11$^{-/-}$, or Gsdmd$^{-/-}$ mice compared to WT and
478 Casp-1$^{-/-}$ BMDMΦ. Finally, we sought to determine the role of IL-1 cytokine responses by
479 MΦ in restricting the replication of *Rickettsia* spp. and showed that transfer of IL-1α$^{-/-}$
480 BMDMΦ, and to much lesser extent the administration of IL-1β$^{-/-}$ BMDMΦ, exacerbated
481 the disease progression in WT mice injected with either pathogenic or non-pathogenic
482 *Rickettsia* spp. It is worth noting that IL-1α is produced by other immune cells, such as
483 neutrophils. Although our study did not evaluate a potential contributing role of

484 neutrophils, preceding findings suggest that neutrophils did not alter the course of
485 rickettsiosis or contributed to the restriction of bacterial growth (Papp et al., 2016).
486 Overall, our findings present a previously unappreciated model of host invasion by which
487 pathogenic, but not non-pathogenic, *Rickettsia* spp. become ubiquitinated, initiate
488 autophagy, but avoid autophagolysosomal destruction, while elude pro-IL-1α induction
489 and diminish IL-1α secretion; likely via the dampening of the Casp-11-Gsdmd signaling
490 pathway, to facilitate their replication in MΦ and ultimately cause host dissemination
491 (Figure 5H).
492

493 **Materials and Methods**

494 **Animals**

495 All experiments were conducted in fully AAALAC accredited program using 8-10 weeks
496 old female C57BL/6J WT mice in a specific pathogen-free environment according to the
497 University of Maryland School of Medicine Institutional Animal Care and Use Committee
498 (IACUC) in compliance with the National Institutes of Health Guide.
499

500 **Antibodies and reagents**

501 Anti(α)-IL-1α (clone ALF-161), αIL-1β (clone B122), or an isotype control IgG (Armenian
502 hamster IgG) antibody (Ab) were purchased from BioXCell. Mono- and polyubiquitinylated
503 conjugated Ab (FK2) (αUb) was obtained from Enzo Life Sciences. Anti-LC3B (E5Q2K)
504 Ab was from Cell Signaling Technology. αCaspase (Casp)-1 Ab was purchased from
505 Adipogen, while αCasp-11 [EPR18628] and αGSDMD [EPR19828] Abs were obtained
506 from Abcam. Elongation factor Ts (EF-Ts) Ab was obtained from Primm Biotech as

507 previously described (Voss et al., 2020). The p62 (SQSTM1) Ab, and 3-methyladenine
508 (3-MA) were purchased from Sigma. LAMP2 (H4B4) and GAPDH (FL-335) Abs were from
509 Santa Cruz Biotechnology. ProLong Gold antifade mounting medium with DAPI (4′,6-
510 diamidino-2-phenylindole), paraformaldehyde (PFA), Halt protease and phosphatase
511 inhibitor cocktail, and Alexa 488/594-conjugated secondary Abs were purchased from
512 Thermo Fisher Scientific. Endotoxin-free recombinant mouse IL-1α and IL-1β proteins
513 were purchased from BioLegend.
514
515 **Bacterial strains, cell culture, and infection**
516 Vero76 cells (African green monkey kidney, ATCC, RL-1587) were maintained in minimal
517 Dulbecco's modified Eagle's medium (DMEM) supplemented with 10% heat-inactivated
518 fetal bovine serum (FBS) at 37°C with 5% CO_2. *R. montanensis* strain M5/6 and *R.*
519 *rickettsia* strain Sheila Smith (*SS*) were obtained from Dr. Ted Hackstadt (Rocky Mountain
520 Laboratories, NIH, MT, USA) and *R. typhi* strain Wilmington was obtained from CDC. All
521 *Rickettsia* strains were propagated in Vero76 cells grown in DMEM supplemented with
522 5% FBS at 34°C with 5% CO_2. All *Rickettsia* were purified as previously described
523 (Rennoll-Bankert et al., 2015). For infection of BMDMΦ, purified *Rickettsia* were used at
524 a multiplicity of infection (MOI) of 50 for various length of times. Rickettsiosis in mice was
525 induced by tail vein injection (*i.v.*) of purified *Rickettsia* (10^5-10^6 PFU), resuspended in
526 PBS. At Days 1, 3, and 7 after administration, blood was collected, and serum cytokine
527 levels were measured by flow cytometry. Splenic tissue specimens were collected at the
528 indicated times and used for bacterial burden analysis by qPCR described below.
529

530 **Differentiation of bone marrow-derived macrophages**

531 Bone marrow cells were isolated from femurs and tibias of WT, ATG5$^{fl/fl}$, ATG5$^{fl/fl}$-LysM-
532 Cre, IL-1α$^{-/-}$, IL-1β$^{-/-}$, Gsdmd$^{-/-}$, Casp-1$^{-/-}$, Casp-11$^{-/-}$, Casp-1/Casp-11$^{-/-}$ mice. Femurs from
533 Casp-1$^{-/-}$, Casp-11$^{-/-}$, Casp-1/Casp-11$^{-/-}$ were kindly provided by Dr. Amal Amer (The Ohio
534 State University, OH, USA), femurs from ATG5$^{fl/fl}$ and ATG5$^{fl/fl}$-LysM-Cre mice were
535 provided by Dr. Christina Stallings (Washington University School of Medicine, MO,
536 USA), while bones from IL-1α$^{-/-}$ and IL-1β$^{-/-}$ mice were obtained from Dr. Thirumala-Devi
537 Kanneganti (St. Jude Children's Research Hospital, TN, USA). Femurs from Gsdmd$^{-/-}$
538 were kindly provided by Dr. Matthew Welch (University of California, Berkeley, CA, USA).
539 Differentiation was induced by culturing bone marrow cells in RPMI 1640 medium
540 supplemented with 10% FBS and 30% L929-conditioned medium (a source of
541 macrophage colony stimulating factor) and cultured for 7 days as described previously
542 (Voss et al., 2016).

543

544 **Measurement of cytokines and chemokines**

545 IL-1 cytokine concentrations in the sera of mice or supernatants from cultured BMDMΦ
546 were assessed using the LEGENDplex mouse inflammation kit (BioLegend) following the
547 manufacturer's instructions as described previously (Voss et al., 2016).

548

549 **RNA isolation and quantitative real-time PCR**

550 BMDMΦ samples were collected at 2, 6, 24, and 48 h post-infection, while spleens were
551 collected at day 3 or 7 post infection. RNA was extracted from 1 x 10^6 BMDMΦ or 100 µl
552 of organ homogenate using the Quick-RNA miniprep kit (ZymoResearch). The iScript

553 Reverse Transcription Supermix kit (Bio-Rad; 1708841) was used to synthesize cDNAs
554 from 200 ng of RNA according to the manufacturer's instructions. Quantitative real-time
555 PCR was performed using SYBR Green (Thermo Fisher Scientific), 2 µl cDNA and 1 µM
556 each of the following oligonucleotides for rickettsial citrate synthase gene (*gltA*) forward
557 (F): 5'-CATAATAGCCATAGGATGAG-3'; reverse (R): 5'-ATGATTTATGGGGAACTACC-
558 3' and analyzed as described previously (Smalley et al., 2016). Oligonucleotides for
559 *GAPDH* were obtained from Qiagen.
560

561 **Immunofluorescence**

562 Eight-well chamber slides were seeded with BMDMΦ and infected with partially
563 purified pathogenic and non-pathogenic *Rickettsia* spp. as described previously (Rennoll-
564 Bankert et al., 2015). Briefly, partially purified *Rickettsia* were added to BMDMΦ and
565 incubated for various length of time at 34°C with 5% CO_2. Following incubation, cells were
566 washed three times with 1 x PBS and fixed with 4% paraformaldehyde (PFA) for 20 min
567 at room temperature. Cells were than permeabilized in blocking buffer (0.3% saponin and
568 0.5% normal goat serum in 1 x PBS) for 30 min and incubated for 1 h with the following
569 primary Abs diluted in Ab dilution buffer (0.3% saponin in 1 x PBS): αEF-Ts (1:500), αUb
570 (1:100), αLC3B (1:100), and αLAMP2 (1:100). Cells were then washed with 1 x PBS and
571 incubated for 1 h with αAlexa Fluor 594 or αAlexa Fluor 488 secondary Abs diluted
572 1:1,500 in Ab dilution buffer. Next, cells were washed with 1 x PBS and mounted with
573 ProLong Gold antifade mounting medium containing DAPI. Images were acquired using
574 the Nikon W-1 spinning disk confocal microscope (University of Maryland Baltimore,

575 Confocal Core Facility) and analyzed using Fiji software. Approximately 100 host cells
576 were enumerated for each experiment and each experiment was repeated five times.
577
578 **Extract preparation, and Western blot analysis.**
579 *Rickettsia*-infected BMDMΦ cells were lysed for 2 h at 4°C in ice-cold lysis buffer (50 mM
580 HEPES [pH 7.4], 137 mM NaCl, 10% glycerol, 1 mM EDTA, 0.5% NP-40, and
581 supplemented with protease and phosphatase inhibitory cocktails) as described
582 previously (9). Equal amounts of protein were loaded for SDS-PAGE and membranes
583 were probed with αp62, αLC3B, αCasp-1, αCasp-11, αGSDMD, αIL-1α, αIL-1β, αEF-Ts,
584 and αGAPDH Abs, followed by enhanced chemiluminescence with secondary Abs
585 conjugated to horseradish peroxidase.
586
587 **Neutralization of endogenous IL-1α and IL-1β**
588 For *in vivo* neutralization of IL-1α and IL-1β, C57BL/6J WT mice were *i.v.* injected with
589 250 mg of αIL-1α (clone ALF-161, BioXCell), αIL-1β (clone B122, BioXCell), or an IgG-
590 isotype control (Armenian hamster IgG, BioXCell) Ab 24 h before the induction of mild
591 rickettsiosis using 10^5 PFU of *R. typhi*, *R. rickettsii*, or *R. montanensis*.
592
593 **Adoptive transfer of bone marrow-derived macrophages**
594 C57BL/6J WT mice were injected (*i.v.*) twice with PBS- or dichloromethylene biphosphate
595 (Cl_2MBP)-liposomes 72 and 48 h prior to macrophage transfer as described previously
596 (Voss et al., 2016). Next, C57BL/6J WT mice were injected (*i.v.*) with WT, IL-1$\beta^{-/-}$, or IL-

597 1α$^{-/-}$ BMDMΦ [5 x 10^6 cells/mouse] followed by infection (24 h post-MΦ transfer) with *R.*
598 *typhi*, *R. rickettsii*, *R. montanensis*, or PBS (dose 10^5 PFU).
599
600 **Statistical analysis**
601 Endpoint studies of mice subjected to mild (10^5 PFU) and severe (10^6 PFU) rickettsiosis
602 were analyzed by using Kaplan-Meir survival curves and the log-rank test (GraphPad
603 Prism Software, version 8). The statistical significance was assessed using ANOVA with
604 Tukey's multiple comparisons post-test (GraphPad). Data are presented as mean ± SEM,
605 unless stated otherwise. Alpha level was set to 0.05.
606
607 **Acknowledgments**
608 We gratefully acknowledge Drs. Amal Amer (The Ohio State University, OH, USA),
609 Thirumala-Devi Kanneganti (St. Jude Children's Research Hospital, TN, USA), Christina
610 Stallings (Washington University School of Medicine, MO, USA), Matthew Welch
611 (University of California, Berkeley, CA, USA) and Ted Hackstadt (Rocky Mountain
612 Laboratories, NIH, MT, USA) for generously providing us with essential biological
613 specimens and reagents, including femurs from various knock-out mice and rickettsial
614 strains. We would like to thank Hodalis Gaytan for her technical assistance in completing
615 some confocal and immunoblot experiments for the manuscript. In addition, we thank
616 Magda Beier-Sexton for her administrative, technical, organizational, and editorial
617 contributions as well as Dr. Stefanie Vogel (University of Maryland School of Medicine,
618 Baltimore, MD, USA) for critical discussions and editorial contributions to the manuscript.

This work was supported with funds from the NIAID/NIH grants (R01AI017828 and R01AI126853 to A.F.A.).

Conflicts of Interest

The authors declare no conflict of interest. The funding sources had no role in the design of the study, in the collection, analyses, or interpretation of data, in the writing of the manuscript, or in the decision to publish the results.

References

Batista, S.J., Still, K.M., Johanson, D., Thompson, J.A., O'Brien, C.A., Lukens, J.R., and Harris, T.H. (2020). Gasdermin-D-dependent IL-1α release from microglia promotes protective immunity during chronic *Toxoplasma gondii* infection. Nature Communications *11*, 1–13.

Bechelli, J., Vergara, L., Smalley, C., Buzhdygan, T.P., Bender, S., Zhang, W., Liu, Y., Popov, V.L., Wang, J., Garg, N., et al. (2018). Atg5 Supports *Rickettsia australis* Infection in Macrophages *In Vitro* and *In Vivo*. Infection and Immunity *87*, 1–19.

Burke, T.P., Engström, P., Chavez, R.A., Fonbuena, J.A., Vance, R.E., and Welch, M.D. (2020). Inflammasome-mediated antagonism of type I interferon enhances *Rickettsia* pathogenesis. Nature Microbiology *5*, 688–696.

Campbell-Valois, F.-X.X., Sachse, M., Sansonetti, P.J., and Parsot, C. (2015). Escape of actively secreting *shigella flexneri* from ATG8/LC3-Positive vacuoles formed during cell-to-cell spread is facilitated by IcsB and VirA. MBio *6*, 1–11.

Curto, P., Simões, I., Riley, S.P., and Martinez, J.J. (2016). Differences in Intracellular Fate of Two Spotted Fever Group *Rickettsia* in Macrophage-Like Cells. Frontiers in Cellular and Infection Microbiology *6*, 1–14.

Engström, P., Burke, T.P., Mitchell, G., Ingabire, N., Mark, K.G., Golovkine, G., Iavarone, A.T., Rape, M., Cox, J.S., and Welch, M.D. (2019). Evasion of autophagy mediated by *Rickettsia* surface protein OmpB is critical for virulence. Nature Microbiology *4*, 2538–2551.

Guillotte, M.L., Gillespie, J.J., Chandler, C.E., Rahman, M.S., Ernst, R.K., and Azad, A.F. (2018). *Rickettsia* lipid A biosynthesis utilizes the late acyltransferase LpxJ for secondary fatty acid addition. Journal of Bacteriology.

Guillotte ML, Chandler CE, Verhoeve VI, Gillespie JJ, Driscoll TP, Rahman MS, Ernst RK, Azad AF. (2021). Lipid A Structural Divergence in *Rickettsia* Pathogens. mSphere. *6*, e00184-21.

654 Jounai, N., Kobiyama, K., Shiina, M., Ogata, K., Ishii, K.J., and Takeshita, F. (2011).
655 NLRP4 Negatively Regulates Autophagic Processes through an Association with Beclin1.
656 The Journal of Immunology *186*, 1646–1655.
657 Kanneganti, A., Malireddi, R.K.S., Saavedra, P.H.V., Walle, L. Vande, Van Gorp, H.,
658 Kambara, H., Tillman, H., Vogel, P., Luo, H.R., Xavier, R.J., et al. (2018). GSD MD is
659 critical for autoinflammatory pathology in a mouse model of Familial Mediterranean Fever.
660 Journal of Experimental Medicine *215*, 1519–1529.
661 Klionsky, D.J., Abdelmohsen, K., Abe, A., Abedin, M.J., Abeliovich, H., Arozena, A.A.,
662 Adachi, H., Adams, C.M., Adams, P.D., Adeli, K., et al. (2016). Guidelines for the use and
663 interpretation of assays for monitoring autophagy (3rd edition). Autophagy.
664 Krakauer, T. (2019). Inflammasomes, Autophagy, and Cell Death: The Trinity of Innate
665 Host Defense against Intracellular Bacteria. Mediators of Inflammation *2019*, 1–10.
666 Lehman, S.S., Noriea, N.F., Aistleitner, K., Clark, T.R., Dooley, C.A., Nair, V., Kaur, S.J.,
667 Rahman, M.S., Gillespie, J.J., Azad, A.F., et al. (2018). The Rickettsial Ankyrin Repeat
668 Protein 2 Is a Type IV Secreted Effector That Associates with the Endoplasmic Reticulum.
669 MBio *9*.
670 Lin, M., Liu, H., Xiong, Q., Niu, H., Cheng, Z., Yamamoto, A., and Rikihisa, Y. (2016).
671 *Ehrlichia* secretes Etf-1 to induce autophagy and capture nutrients for its growth through
672 RAB5 and class III phosphatidylinositol 3-kinase. Autophagy *12*, 2145–2166.
673 Liu, X., Zhang, Z., Ruan, J., Pan, Y., Magupalli, V.G., Wu, H., and Lieberman, J. (2016).
674 Inflammasome-activated gasdermin D causes pyroptosis by forming membrane pores.
675 Nature *535*, 153–158.
676 Malik, A., and Kanneganti, T.-D. (2018). Function and regulation of IL-1α in inflammatory
677 diseases and cancer. Immunological Reviews *281*, 124–137.
678 Mitchell, G., and Isberg, R.R. (2017). Innate Immunity to Intracellular Pathogens:
679 Balancing Microbial Elimination and Inflammation. Cell Host and Microbe *22*, 166–175.
680 Moderzynski, K., Papp, S., Rauch, J., Heine, L., Kuehl, S., Richardt, U., Fleischer, B., and
681 Osterloh, A. (2016). CD4+T Cells Are as Protective as CD8+T Cells against *Rickettsia*
682 *typhi* Infection by Activating Macrophage Bactericidal Activity. PLoS Neglected Tropical
683 Diseases *10*.
684 Ogawa, M., Yoshimori, T., Suzuki, T., Sagara, H., Mizushima, N., and Sasakawa, C.
685 (2005). Escape of intracellular *Shigella* from autophagy. Science.
686 Papp, S., Moderzynski, K., Rauch, J., Heine, L., Kuehl, S., Richardt, U., Mueller, H.,
687 Fleischer, B., and Osterloh, A. (2016). Liver Necrosis and Lethal Systemic Inflammation
688 in a Murine Model of *Rickettsia typhi* Infection: Role of Neutrophils, Macrophages and NK
689 Cells. PLoS Neglected Tropical Diseases *10*, e0004935.
690 Personnic, N., Bärlocher, K., Finsel, I., and Hilbi, H. (2016). Subversion of Retrograde
691 Trafficking by Translocated Pathogen Effectors. Trends in Microbiology *24*, 450–462.
692 Place, D.E., and Kanneganti, T.D. (2018). Recent advances in inflammasome biology.
693 Current Opinion in Immunology *50*, 32–38.
694 Rahman, M.S., Ammerman, N.C., Sears, K.T., Ceraul, S.M., and Azad, A.F. (2010).
695 Functional characterization of a phospholipase A2 homolog from *Rickettsia typhi*. Journal
696 of Bacteriology *192*, 3294–3303.
697 Rahman, M.S., Gillespie, J.J., Kaur, S.J., Sears, K.T., Ceraul, S.M., Beier-Sexton, M.,
698 and Azad, A.F. (2013). *Rickettsia typhi* Possesses Phospholipase A2 Enzymes that Are
699 Involved in Infection of Host Cells. PLoS Pathogens *9*, e1003399.

700 Ray, K., Marteyn, B., Sansonetti, P.J., and Tang, C.M. (2009). Life on the inside: The
701 intracellular lifestyle of cytosolic bacteria. Nature Reviews Microbiology *7*, 333–340.
702 Rennoll-Bankert, K.E., Rahman, M.S., Gillespie, J.J., Guillotte, M.L., Kaur, S.J., Lehman,
703 S.S., Beier-Sexton, M., and Azad, A.F. (2015). Which Way In? The RalF Arf-GEF
704 Orchestrates *Rickettsia* Host Cell Invasion. PLoS Pathogens *11*, 1–28.
705 Rennoll-Bankert, K.E., Rahman, M.S., Guillotte, M.L., Lehman, S.S., Beier-Sexton, M.,
706 Gillespie, J.J., and Azad, A.F. (2016). RalF-mediated activation of Arf6 controls *Rickettsia*
707 *typhi* invasion by co-opting phosphoinositol metabolism. Infection and Immunity *84*,
708 3496–3506.
709 Rikihisa, Y. (2017). Role and function of the type IV secretion system in *Anaplasma* and
710 *Ehrlichia* species. In Current Topics in Microbiology and Immunology, pp. 297–321.
711 Rikihisa, Y. (2019). Subversion of RAB5-regulated autophagy by the intracellular
712 pathogen *Ehrlichia chaffeensis*. Small GTPases *10*, 343–349.
713 Rikihisa, Y., and Lin, M. (2010). Anaplasma phagocytophilum and *Ehrlichia chaffeensis*
714 type IV secretion and Ank proteins. Curr Opin Microbiol *13*, 59–66.
715 Rumfield, C., Hyseni, I., McBride, J.W., Walker, D.H., and Fang, R. (2020). Activation of
716 ASC inflammasome driven by toll-like receptor 4 contributes to host immunity against
717 rickettsial infection. Infection and Immunity *88*.
718 Sahni, A., Fang, R., Sahni, S.K., and Walker, D.H. (2018). Pathogenesis of Rickettsial
719 Diseases: Pathogenic and Immune Mechanisms of an Endotheliotropic Infection. Annual
720 Review of Pathology: Mechanisms of Disease *14*, 127–152.
721 Seveau, S., Turner, J., Gavrilin, M.A., Torrelles, J.B., Hall-Stoodley, L., Yount, J.S., and
722 Amer, A.O. (2018). Checks and Balances between Autophagy and Inflammasomes
723 during Infection. Journal of Molecular Biology *430*, 174–192.
724 Smalley, C., Bechelli, J., Rockx-Brouwer, D., Saito, T., Azar, S.R., Ismail, N., Walker,
725 D.H., and Fang, R. (2016). *Rickettsia australis* activates inflammasome in human and
726 murine macrophages. PLoS ONE *11*, 1–20.
727 Storek, K.M., and Monack, D.M. (2015). Bacterial recognition pathways that lead to
728 inflammasome activation. Immunological Reviews.
729 Sun, Q., Fan, J., Billiar, T.R., and Scott, M.J. (2017). Inflammasome and Autophagy
730 Regulation: A Two-way Street. Molecular Medicine *23*, 188–195.
731 Takahama, M., Akira, S., and Saitoh, T. (2018). Autophagy limits activation of the
732 inflammasomes. Immunological Reviews *281*, 62–73.
733 Tapia, V.S., Daniels, M.J.D., Palazón-Riquelme, P., Dewhurst, M., Luheshi, N.M., Rivers-
734 Auty, J., Green, J., Redondo-Castro, E., Kaldis, P., Lopez-Castejon, G., et al. (2019). The
735 three cytokines IL-1β, IL-18, and IL-1α share related but distinct secretory routes. Journal
736 of Biological Chemistry *294*, 8325–8335.
737 Tsuchiya, K., Hosojima, S., Hara, H., Kushiyama, H., Mahib, M.R., Kinoshita, T., and
738 Suda, T. (2021). Gasdermin D mediates the maturation and release of IL-1α downstream
739 of inflammasomes. Cell Reports *34*, 108887.
740 Vladimer, G.I., Marty-Roix, R., Ghosh, S., Weng, D., and Lien, E. (2013). Inflammasomes
741 and host defenses against bacterial infections. Current Opinion in Microbiology.
742 Voss, O.H., and Rahman, M.S. (2021). *Rickettsia*-host interaction: strategies of
743 intracytosolic host colonization. Pathogens and Disease *79*.
744 Voss, O.H., Murakami, Y., Pena, M.Y., Lee, H.-N., Tian, L., Margulies, D.H., Street, J.M.,
745 Yuen, P.S.T., Qi, C.-F., Krzewski, K., et al. (2016). Lipopolysaccharide-Induced CD300b

Receptor Binding to Toll-like Receptor 4 Alters Signaling to Drive Cytokine Responses that Enhance Septic Shock. Immunity *44*, 1365–1378.
Voss, O.H., Gillespie, J.J., Lehman, S.S., Rennoll, S.A., Beier-Sexton, M., Rahman, M.S., and Azad, A.F. (2020). Risk1, a phosphatidylinositol 3-kinase effector, promotes *Rickettsia typhi* intracellular survival. MBio *11*, 1–22.
Wiggins, K.A., Parry, A.J., Cassidy, L.D., Humphry, M., Webster, S.J., Goodall, J.C., Narita, M., and Clarke, M.C.H. (2019). IL-1α cleavage by inflammatory caspases of the noncanonical inflammasome controls the senescence-associated secretory phenotype. Aging Cell *18*, 1–13.
Xue, Y., Enosi Tuipulotu, D., Tan, W.H., Kay, C., and Man, S.M. (2019). Emerging Activators and Regulators of Inflammasomes and Pyroptosis. Trends in Immunology *40*, 1035–1052.
Yu, J., Nagasu, H., Murakami, T., Hoang, H., Broderick, L., Hoffman, H.M., and Horng, T. (2014). Inflammasome activation leads to Caspase-1-dependent mitochondrial damage and block of mitophagy. Proceedings of the National Academy of Sciences *111*, 15514–15519.
Zheng, D., Liwinski, T., and Elinav, E. (2020). Inflammasome activation and regulation: toward a better understanding of complex mechanisms. Cell Discovery *6*, 36.

Figure Legend

Figure. 1. *In vivo* models of rickettsiosis.

(**A**) *Rickettsia* spp. and their level of pathogenicity to humans (Sahni et al., 2018; Voss and Rahman, 2021).

(**B-D**) Establishment of a model of rickettsiosis (LD_{25} and LD_{50}) for *R. typhi* [B], *R. rickettsii* [C] or *R. montanensis* [D] in C57BL/6J WT mice. Animals were injected via tail vein (*i.v.*) with different doses [10^5-10^6 PFU] of *R. typhi*, *R. rickettsii*, *R. montanensis*, or PBS (n=12 for each treatment). Survival was monitored for 7 days.

(**E**) Bacterial burden was tested in spleens of *R. typhi*-, *R. rickettsii*-, *R. montanensis*-, or PBS-injected WT mice (n=5 per each treatment) shown in (B-D) by *GltA* RT-qPCR at day 3 and 7 (n=5 for each treatment) using the host housekeeping gene, *Gapdh*, for normalization.

778 (**F-G**) Serum samples from rickettsiae-infected mice described in (B-D) were analyzed for
779 IL-1β (F) and IL-1α (G) production using the Legendplex kits (BioLegend) followed by flow
780 cytometry analysis.
781 Error bars in (E-G) represent means ± SEM from five independent experiments; NS, non-
782 significant; *$p \leq 0.05$; **$p \leq 0.01$; ***$p \leq 0.001$; ****$p \leq 0.005$.
783
784 **Figure. 2. Neutralization of IL-1α activity augments mortality of pathogenic and**
785 **non-pathogenic *Rickettsia*-induced rickettsiosis.**
786 (**A-C**) C57BL/6J WT mice were injected via tail vein (*i.v.*) with 10^5 PFU of *R. typhi* [A], *R.*
787 *rickettsii* [B], *R. montanensis* [C], or PBS (A-C; n=12 for each treatment) followed by a
788 subsequent injection (*i.v.*) with αIL-1β, αIL-1α or IgG-isotype control antibody (Ab) [250
789 μg Ab/mouse]. Survival was monitored for 7 days.
790 (**D**) Bacterial burden was tested in spleens of Ab-treated *R. typhi*-, *R. rickettsii*-, *R.*
791 *montanensis*-, or PBS-injected WT mice shown in (A-C) by *GltA* RT-qPCR at day 7 (n=5
792 for each treatment) using the host housekeeping gene, *Gapdh*, for normalization.
793 (**E-F**) Serum samples from mice described in (A-C) were analyzed for IL-1β (E) and IL-
794 1α (F) production at day 7 (n=5 for each treatment) using the Legendplex kits (BioLegend)
795 followed by flow cytometry analysis.
796 Error bars in (D-F) represent means ± SEM from five independent experiments; NS, non-
797 significant; *$p \leq 0.05$; **$p \leq 0.01$; ***$p \leq 0.001$; ****$p \leq 0.005$.
798
799 **Figure. 3. Pathogenic, but not non-pathogenic, *Rickettsia* species limit Caspase-1-**
800 **and Caspase-11-dependent IL-1 signaling to facilitate their intracellular replication**
801 **in macrophages.**

802 (**A-I**) BMDMΦ from WT, Casp-1$^{-/-}$, Casp-11$^{-/-}$, or Casp-1/11$^{-/-}$ mice were infected with *R.*
803 *typhi* (A-C), *R. rickettsii* (D-F) or *R. montanensis* (G-I) [MOI=50] for 0, 6, 24, and 48 h.
804 Culture supernatants were analyzed for production of IL-1β (A, D, G) and IL-1α (B, E, H)
805 using Legendplex kits (BioLegend) followed by flow cytometry. BMDM cell death at 24 h
806 post-infection, was measured by LDH release assay (C, F, I).
807 (**J**) Bacterial burdens in infected BMDMΦ were evaluated 2 and 24 h post-infection by
808 *GltA* RT-qPCR. Expression of the host housekeeping gene *Gapdh* was used for
809 normalization.
810 (**K**) Western analysis of Casp-1, Casp-11, and GSDMD induction and processing at 24 h
811 post-infection with *R. typhi*, *R. rickettsii*, or *R. montanensis* using αCasp-1, αCasp-11, and
812 αGSDMD antibodies. Reblotting with rickettsial specific αEF-Ts and host cell specific
813 αGAPDH antibodies served as infection and equal loading controls respectively.
814 Error bars in (G) represent means ± SEM from five independent experiments; NS: non-
815 significant; *$p \leq 0.05$; **$p \leq 0.01$; ***$p \leq 0.005$. Immunoblot data are a representative of
816 three independent experiments.
817
818 **Figure. 4. Pathogenic *Rickettsia* species induce autophagy and evade**
819 **autophagolysosomal destruction to establish a replication niche in macrophages.**
820 BMDMΦ from ATG5$^{fl/fl}$ or ATG5$^{fl/fl}$-LysM-Cre mice were infected with *R. typhi*, *R. rickettsii*,
821 or *R. montanensis* [MOI=50] for 2 h.
822 (**A-C**) *Rickettsia*-infected ATG5$^{fl/fl}$ and ATG5-deficient BMDMΦ were fixed with 4% PFA
823 and *Rickettsia* spp. were detected using the rickettsial specific Alexa Fluor 594-

824 conjugated EF-Ts, while LC3B, and Lamp2 expression was assessed using Alexa Fluor
825 488-conjuagted αLC3B, or αLamp2 antibodies respectively.
826 (**D**) Graphs show the numbers of engulfment of cells in which *Rickettsia* spp. colocalized
827 with LC3B, or Lamp2. DNA was stained using DAPI (blue). Colocalization data were
828 analyzed using Coloc 2 plugin Fiji software. Bars in panels A-C, 10 μm.
829 (**E**) Culture supernatants of *Rickettsia*-infected $ATG5^{fl/fl}$ and ATG5-deficient BMDMΦ were
830 analyzed 24 h post-infection for the production of IL-1β and IL-1α using Legendplex kits
831 (BioLegend) followed by flow cytometry.
832 Error bars (D, E) represent means ± SEM from five independent experiments; NS: non-
833 significant; $*p \leq 0.05$; $**p \leq 0.01$; $***p \leq 0.005$.
834
835 **Figure. 5. Macrophages-dependent secretion of IL-1α contributes more than IL-1β**
836 **for controlling the survival and dissemination of pathogenic and non-pathogenic**
837 ***Rickettsia* species.**
838 (**A-D**) Dichloromethylene biphosphate (Cl_2MBP)-treated C57BL/6J WT mice were
839 injected *i.v.* with WT, IL-$1\beta^{-/-}$, or IL-$1\alpha^{-/-}$ BMDMΦ [5 x 10^6 cells/mouse] followed by infection
840 (24 h post-MΦ transfer) with *R. typhi* [B], *R. rickettsii* [C], or *R. montanensis* [D] (dose 10^5
841 PFU) (B-D; n=12 for each treatment). Survival was monitored for 7 days.
842 (**E**) Bacterial burden was tested in spleens from mice described in (A-D) by *GltA* RT-
843 qPCR at day 7 (n=5 for each treatment) using the housekeeping gene, *Gapdh*, for
844 normalization.

845 (**F-G**) Serum samples from mice described in (B-D) were analyzed for IL-1β (F) and IL-
846 1α (G) production at day 7 (n=5 for each treatment) using the Legendplex kits (BioLegend)
847 followed by flow cytometry analysis.
848 Error bars in (E-G) represent means ± SEM from five independent experiments; NS, non-
849 significant; *$p \leq 0.05$; **$p \leq 0.01$; ***$p \leq 0.001$; ****$p \leq 0.005$.
850 (**H**) Proposed working model on how pathogenic *Rickettsia* spp. become ubiquitinated,
851 induce autophagy, and escape autophagolysosomal destruction, while dampen Casp-1
852 and Casp-11-dependent IL-1 signaling responses to establish a replication niche in MΦ
853 and ultimately causing host dissemination. However, non-pathogenic *Rickettsia* spp.
854 likely get destroyed by phagolysomal fusion that may induce inflammasome mediated IL-
855 1 response.
856
857 **Fig. S1. Splenic data during infection of pathogenic and non-pathogenic *Rickettsia***
858 **species.**
859 (**A**) Representative images of spleens (at day 7) from C57BL/6J WT mice injected *i.v.*
860 with *R. typhi*, *R. rickettsii*, *R. montanensis*, or PBS (dose 10^6 PFU).
861 (**B**) Spleen weight from injected animals was evaluated at day 7 day (n=5).
862 Error bars in (B) represent means ± SEM from five independent experiments; *$p \leq 0.05$;
863 ***$p \leq 0.001$.
864
865 **Fig. S2. Splenic data after IL-1 signaling neutralization during infection of**
866 **pathogenic and non-pathogenic *Rickettsia* species.**

867 (**A**) Representative images of spleens (day 7) from C57BL/6J WT mice injected *i.v.* with
868 *R. typhi*, *R. rickettsii*, *R. montanensis*, or PBS (dose 10^5 PFU) followed by administration
869 of αIL-1β, αIL-1α, or IgG isotype control antibody (Ab) [250 μg Ab/mouse] (24 h post-Ab
870 injection).
871 (**B**) Spleen weight from injected animals was evaluated at day 7 (n=5).
872 Error bars in (B) represent means ± SEM from five independent experiments; *$p \leq 0.05$;
873 **$p \leq 0.01$; ***$p \leq 0.001$.
874
875 **Fig. S3. Administration of recombinant IL-1α rescues fatal *Rickettsia*-induced**
876 **rickettsiosis.**
877 (**A-C**) C57BL/6J WT mice were injected *i.v.* with recombinant (r)IL-1β or rIL-1α protein
878 [500 ng/mouse] followed by infection (24 h post protein injection) with 10^6 PFU of *R. typhi*
879 [A], *R. rickettsii* [B], *R. montanensis* [C], or PBS (A-C; n=15 for each treatment). Survival
880 was monitored for 7 days.
881 (**D**) Bacterial burden was tested in spleens of protein-treated, *R. typhi*-, *R. rickettsii*-, *R.*
882 *montanensis*- or PBS-injected WT mice shown in (A-C) by *GltA* RT-qPCR at day 7 (n=5
883 for each treatment) using the housekeeping gene, *Gapdh*, for normalization.
884 (**E**) Representative images of spleens from C57BL/6J WT mice injected *i.v.* with rIL-1β or
885 rIL-1α protein followed by administration of *R. typhi*, *R. rickettsii*, *R. montanensis* or PBS
886 (dose 10^6 PFU) at day 7.
887 (**F**) Spleen weight from injected animals was evaluated at day 7 day (n=5).

888 (**G-H**) Serum samples from mice described in (A-C) were analyzed for IL-1β (G) and IL-
889 1α (H) production at day 7 (n=5 for each treatment) using the Legendplex kits (BioLegend)
890 followed by flow cytometry analysis.
891 Error bars in (D, F-H) represent means ± SEM from five independent experiments; NS,
892 non-significant; *$p \leq 0.05$; **$p \leq 0.01$; ***$p \leq 0.001$; ****$p \leq 0.005$.
893
894 **Fig. S4. IL-1α, but not IL-1β, contributes to the survival of *Rickettsia* species in**
895 **macrophages.**
896 (**A**-**F**) BMDMΦ from WT, IL-1β$^{-/-}$, or IL-1α$^{-/-}$ mice were infected with *R. typhi*, *R. rickettsii*,
897 or *R. montanensis* [MOI=50] for 0, 6, 24, and 48 h. Culture supernatants were analyzed
898 for production of IL-1β (A, C and E) and IL-1α (B, D and F) using Legendplex kits
899 (BioLegend) followed by flow cytometry.
900 (**G**) Bacterial burden in rickettsiae-infected BMDMΦ from WT, IL-1β$^{-/-}$, or IL-1α$^{-/-}$ mice was
901 evaluated at 2 and 24 h post-infection by *GltA* RT-qPCR. Expression of the housekeeping
902 gene *Gapdh* was used for normalization.
903 (**H**) BMDMΦ from WT mice were either left uninfected (-) or infected with *R. typhi*, *R.*
904 *rickettsii*, or *R. montanensis*, [MOI=50] for 24 h. Lysates were immunoblotted with αIL-1α,
905 αIL-1β, αET-Ts, and αGAPDH antibodies. Densitometry was performed using Fiji
906 software and data represent the fold-change ratios of pro-IL-1β/GAPDH or pro-IL-
907 1α/GAPDH between uninfected and infected cells are shown. Immunoblot data are a
908 representative of three independent experiments.
909 Error bars in (A-G) represent means ± SEM from five independent experiments; NS: non-
910 significant; *$p \leq 0.05$; **$p \leq 0.01$; ***$p \leq 0.005$; ****$p \leq 0.001$.

911

912 **Fig. S5. Gsdmd is involved in the release of IL-1α and IL-1b by macrophages upon**

913 ***Rickettsia* infection.**

914 (**A-B**) BMDMΦ from WT and Gsdmd$^{-/-}$ mice were infected with *R. typhi*, *R. rickettsii*, or *R.*

915 *montanensis* [MOI=50] for 24 h. Culture supernatants were analyzed for production of IL-

916 1β (A) and IL-1α (B) using Legendplex kits (BioLegend) followed by flow cytometry.

917 (**C**) Bacterial burden in rickettsiae-infected BMDMΦ from WT and Gsdmd$^{-/-}$ mice was

918 evaluated at 2 and 24 h post-infection by *GltA* RT-qPCR. Expression of the housekeeping

919 gene *Gapdh* was used for normalization.

920 Error bars in (A-C) represent means ± SEM from five independent experiments; NS: non-

921 significant; *$p \leq 0.05$; **$p \leq 0.01$; ***$p \leq 0.005$.

922

923 **Fig. S6. Pathogenic, but no non-pathogenic, *Rickettsia* species become**

924 **ubiquitinated and induces autophagy in macrophages upon infection.**

925 BMDMΦ from WT mice were infected with *R. typhi*, *R. rickettsii*, or *R. montanensis*

926 [MOI=50] for 2 h.

927 (**A-B**) *Rickettsia*-infected WT BMDMΦ were fixed with 4% PFA, while *Rickettsia* spp. and

928 their ubiquitination status was detected using a rickettsial specific Alexa Fluor 594-

929 conjugated EF-Ts and Alexa Fluor 488-conjuagted αUb antibody respectively.

930 Graph in (B) shows the numbers of ubiquitin positive (Ub^{+}) engulfment *Rickettsia* spp.

931 DNA was stained using DAPI (blue). Colocalization data were analyzed using Coloc 2

932 plugin Fiji software. Bars in panel A, 10 μm.

933 (**C**) BMDMΦ from WT mice were either left uninfected (-) or infected with *R. typhi*, *R.*
934 *rickettsii*, or *R. montanensis*, [MOI=50] for 24 h. Lysates were immunoblotted with αp62,
935 αLC3B, αET-Ts, and αGAPDH antibodies.
936 Densitometry was performed using Fiji software and data represent the fold-change ratios
937 of p62/GAPDH or LC3B/GAPDH between uninfected and infected cells are shown.
938 Immunoblot data are a representative of three independent experiments.
939 Error bars in (B) represent means ± SEM from five independent experiments; $^{**}p \leq 0.01$.
940

941 **Fig. S7. Pharmacological modulation of autophagy regulates the ability of**
942 ***Rickettsia* species to evade autophagolysosomal destruction and their ability to**
943 **establish a replication niche in macrophages.**
944 (**A-F**) BMDMΦ from WT mice were either left untreated (NT; A-C) or pretreated with 3-
945 methyladenine (3-MA, 5 mM; D-F) for 1 h followed by *R. typhi*, *R. rickettsii*, or *R.*
946 *montanensis* [MOI=50] infection for additional 2 h. *Rickettsia*-infected WT BMDMΦ
947 [described in (A-F)] were fixed with 4% PFA and *Rickettsia* spp. were detected using a
948 rickettsial specific Alexa Fluor 594-conjugated EF-Ts Ab, while LC3B, and Lamp2
949 expression was assessed using Alexa Fluor 488-conjuagted αLC3B, or αLamp2 antibody
950 respectively.
951 (**G**) Graph shows the numbers of engulfment of cells in which *Rickettsia* spp. colocalized
952 with either LC3B, or Lamp2. DNA was stained using DAPI (blue). Colocalization data
953 were analyzed using Coloc 2 plugin Fiji software. Bars in panels (A-I), 10 μm.
954 Error bars (G) represent means ± SEM from five independent experiments; NS: non-
955 significant; $^{**}p \leq 0.01$.

956

957 **Fig. S8. Survival and splenic data after adoptive transfer of WT, IL-1β$^{-/-}$, or IL-1α$^{-/-}$**
958 **macrophages and infection of pathogenic and non-pathogenic *Rickettsia* species**
959 **into PBS- or dichloromethylene biphosphate (Cl_2MBP)-treated C57BL/6J WT mice.**
960 (**A-D**) PBS-treated C57BL/6J WT mice were injected *i.v.* with WT, IL-1β$^{-/-}$, or IL-1α$^{-/-}$
961 BMDMΦ [5 x 10^6 cells/mouse] followed by infection (24 h post-MΦ transfer) with *R. typhi*
962 [B], *R. rickettsii* [C], *R. montanensis* [D], or PBS (dose 10^5 PFU) (B-D; n=12 for each
963 treatment). Survival was monitored for 7 days.
964 (**E**) Representative images of spleens (day 7) from PBS- or Cl_2MBP-treated C57BL/6J
965 WT mice injected *i.v.* with WT, IL-1α$^{-/-}$, or IL-1β$^{-/-}$BMDMΦ [5 x 10^6 cells/mouse] followed
966 by administration (24 h post-MΦ transfer) of *R. typhi*, *R. rickettsii*, *R. montanensis*, or PBS
967 (dose 10^5 PFU).
968 (**F**) Spleen weight from injected animals was evaluated at day 7 (n=5).
969 Error bars in (F) represent means ± SEM; from five independent experiments; NS, non-
970 significant; *$p \leq 0.05$; **$p \leq 0.01$.
971
972

Fig. 1

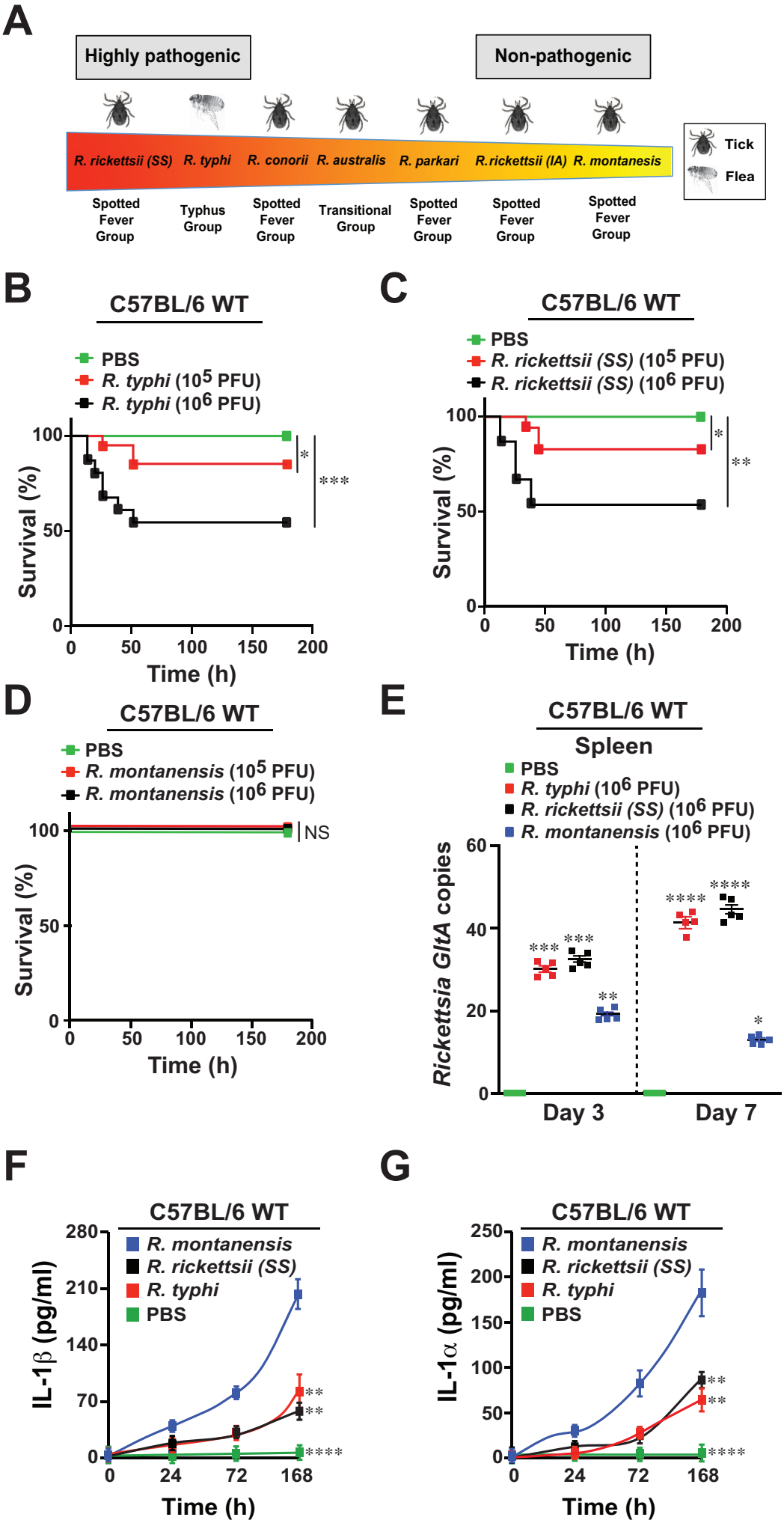
A
Highly pathogenic
Non-pathogenic
R. rickettsii (SS)
R. typhi
R. conorii
R. australis
R. parkari
R.rickettsii (IA)
R. montanesis
Tick
Flea
Spotted Fever Group
Typhus Group
Spotted Fever Group
Transitional Group
Spotted Fever Group
Spotted Fever Group
Spotted Fever Group
B
C57BL/6 WT
PBS
R. typhi (10^5 PFU)
R. typhi (10^6 PFU)
Survival (%)
Time (h)
C
C57BL/6 WT
PBS
R. rickettsii (SS) (10^5 PFU)
R. rickettsii (SS) (10^6 PFU)
Survival (%)
Time (h)
D
C57BL/6 WT
PBS
R. montanensis (10^5 PFU)
R. montanensis (10^6 PFU)
NS
Survival (%)
Time (h)
E
C57BL/6 WT
Spleen
PBS
R. typhi (10^6 PFU)
R. rickettsii (SS) (10^6 PFU)
R. montanensis (10^6 PFU)
Rickettsia GltA copies
Day 3
Day 7
F
C57BL/6 WT
R. montanensis
R. rickettsii (SS)
R. typhi
PBS
IL-1β (pg/ml)
Time (h)
G
C57BL/6 WT
R. montanensis
R. rickettsii (SS)
R. typhi
PBS
IL-1α (pg/ml)
Time (h)

Fig. 2

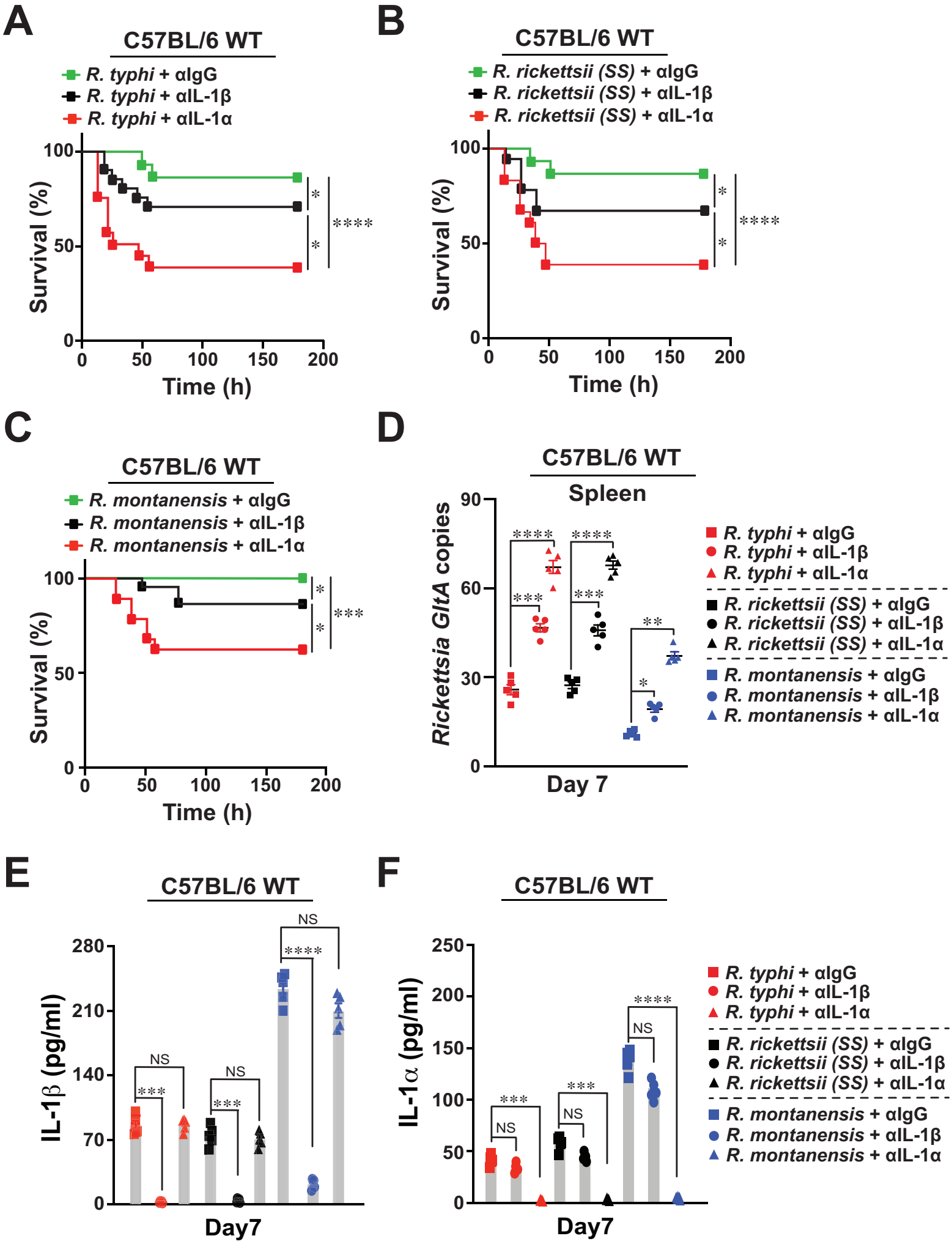
A
C57BL/6 WT
R. typhi + αIgG
R. typhi + αIL-1β
R. typhi + αIL-1α
Survival (%)
Time (h)
B
C57BL/6 WT
R. rickettsii (SS) + αIgG
R. rickettsii (SS) + αIL-1β
R. rickettsii (SS) + αIL-1α
Survival (%)
Time (h)
C
C57BL/6 WT
R. montanensis + αIgG
R. montanensis + αIL-1β
R. montanensis + αIL-1α
Survival (%)
Time (h)
D
C57BL/6 WT
Spleen
Rickettsia GltA copies
Day 7
R. typhi + αIgG
R. typhi + αIL-1β
R. typhi + αIL-1α
R. rickettsii (SS) + αIgG
R. rickettsii (SS) + αIL-1β
R. rickettsii (SS) + αIL-1α
R. montanensis + αIgG
R. montanensis + αIL-1β
R. montanensis + αIL-1α
E
C57BL/6 WT
IL-1β (pg/ml)
Day7
F
C57BL/6 WT
IL-1α (pg/ml)
Day7
R. typhi + αIgG
R. typhi + αIL-1β
R. typhi + αIL-1α
R. rickettsii (SS) + αIgG
R. rickettsii (SS) + αIL-1β
R. rickettsii (SS) + αIL-1α
R. montanensis + αIgG
R. montanensis + αIL-1β
R. montanensis + αIL-1α

Fig. 3

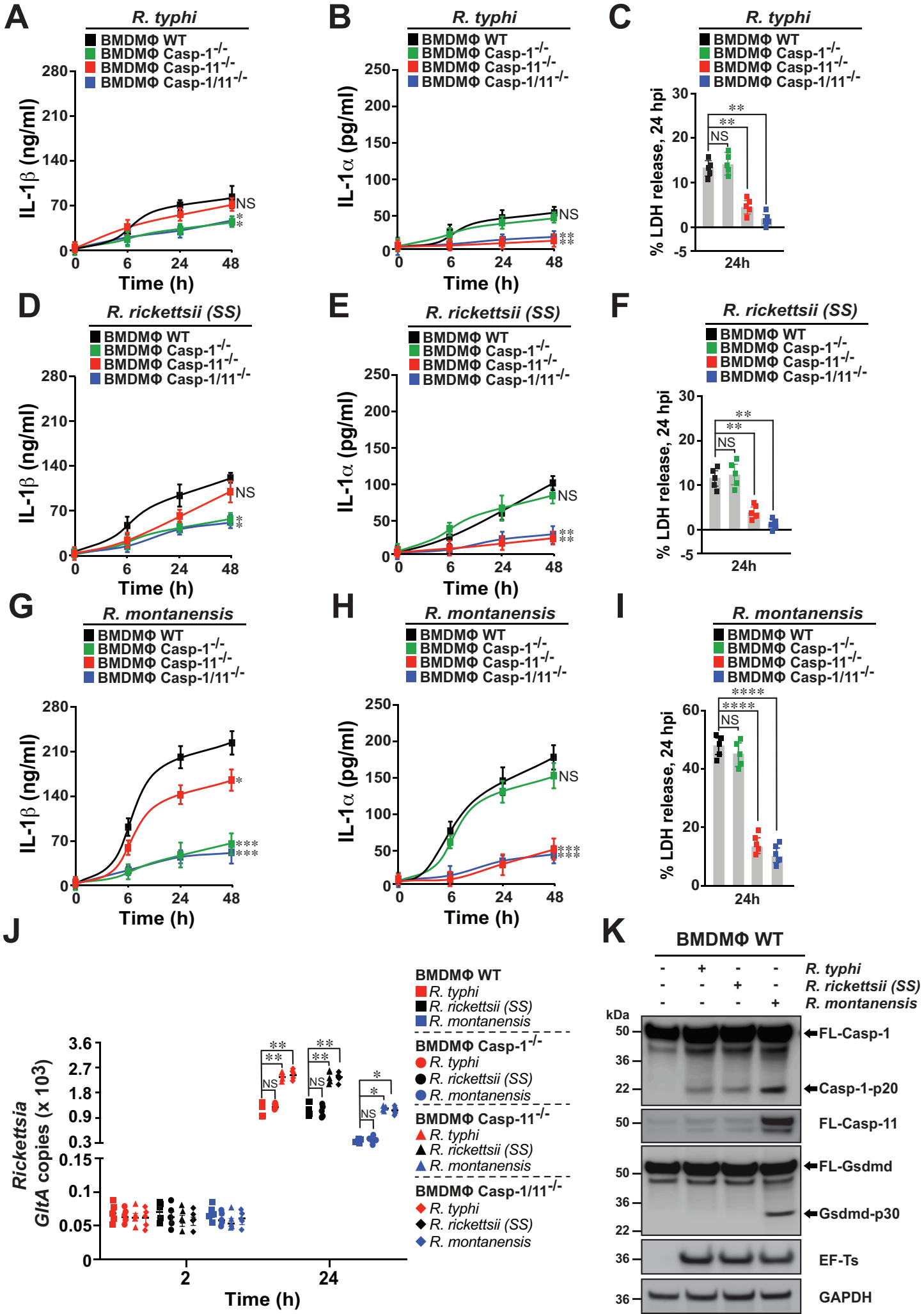
A
R. typhi
BMDMΦ WT
BMDMΦ Casp-1-/-
BMDMΦ Casp-11-/-
BMDMΦ Casp-1/11-/-
IL-1β (ng/ml)
Time (h)
B
R. typhi
IL-1α (pg/ml)
Time (h)
C
R. typhi
% LDH release, 24 hpi
24h
D
R. rickettsii (SS)
IL-1β (ng/ml)
Time (h)
E
R. rickettsii (SS)
IL-1α (pg/ml)
Time (h)
F
R. rickettsii (SS)
% LDH release, 24 hpi
24h
G
R. montanensis
IL-1β (ng/ml)
Time (h)
H
R. montanensis
IL-1α (pg/ml)
Time (h)
I
R. montanensis
% LDH release, 24 hpi
24h
J
Rickettsia GltA copies (x 10^3)
Time (h)
BMDMΦ WT
R. typhi
R. rickettsii (SS)
R. montanensis
BMDMΦ Casp-1-/-
BMDMΦ Casp-11-/-
BMDMΦ Casp-1/11-/-
K
BMDMΦ WT
R. typhi
R. rickettsii (SS)
R. montanensis
kDa
FL-Casp-1
Casp-1-p20
FL-Casp-11
FL-Gsdmd
Gsdmd-p30
EF-Ts
GAPDH

Fig. 5

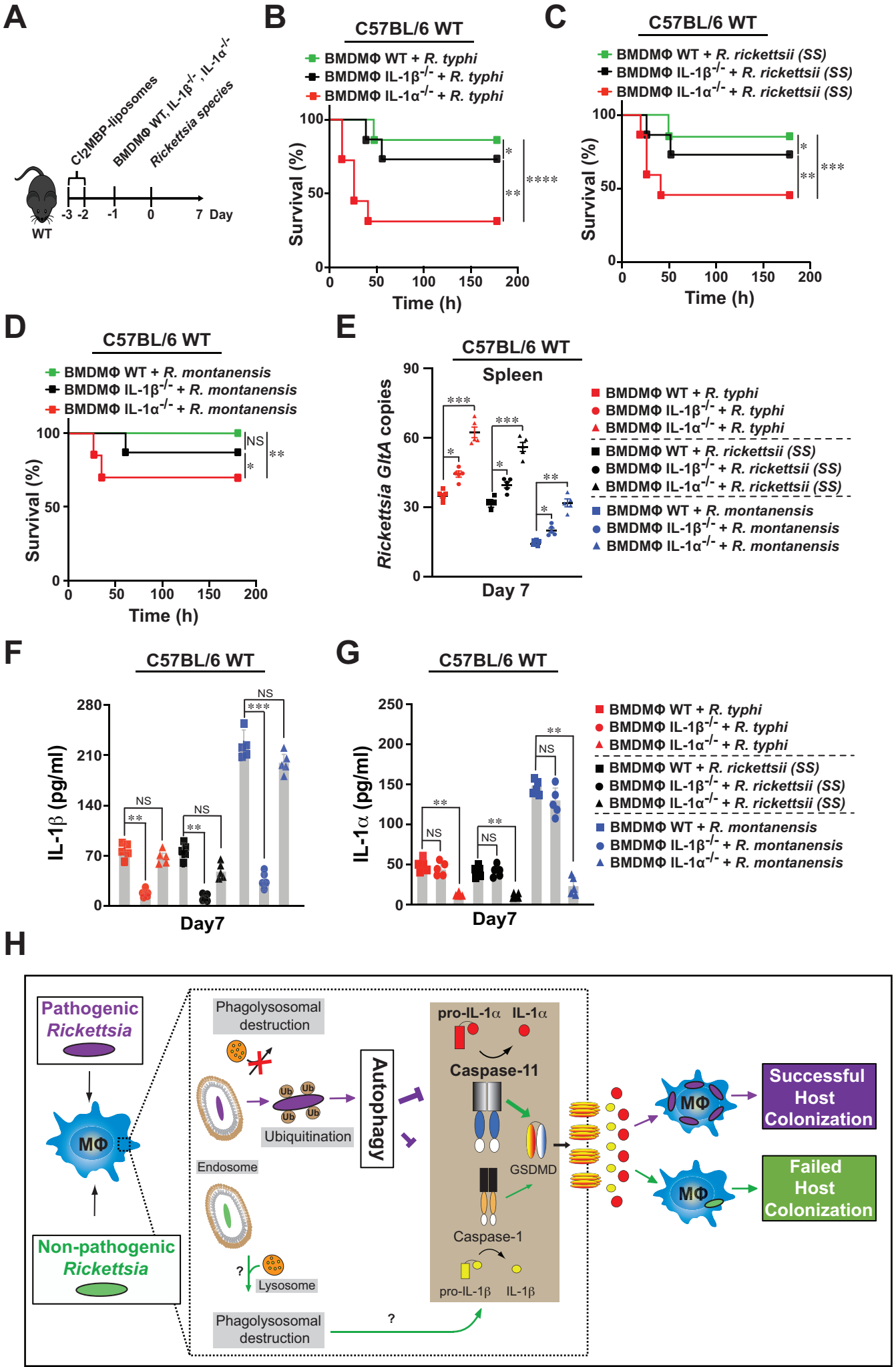
A
Cl2MBP-liposomes
BMDMΦ WT, IL-1β-/-, IL-1α-/-
Rickettsia species
WT
-3 -2 -1 0 7 Day
B
C57BL/6 WT
BMDMΦ WT + R. typhi
BMDMΦ IL-1β-/- + R. typhi
BMDMΦ IL-1α-/- + R. typhi
Survival (%)
Time (h)
C
C57BL/6 WT
BMDMΦ WT + R. rickettsii (SS)
BMDMΦ IL-1β-/- + R. rickettsii (SS)
BMDMΦ IL-1α-/- + R. rickettsii (SS)
Survival (%)
Time (h)
D
C57BL/6 WT
BMDMΦ WT + R. montanensis
BMDMΦ IL-1β-/- + R. montanensis
BMDMΦ IL-1α-/- + R. montanensis
Survival (%)
Time (h)
E
C57BL/6 WT
Spleen
Rickettsia GltA copies
Day 7
BMDMΦ WT + R. typhi
BMDMΦ IL-1β-/- + R. typhi
BMDMΦ IL-1α-/- + R. typhi
BMDMΦ WT + R. rickettsii (SS)
BMDMΦ IL-1β-/- + R. rickettsii (SS)
BMDMΦ IL-1α-/- + R. rickettsii (SS)
BMDMΦ WT + R. montanensis
BMDMΦ IL-1β-/- + R. montanensis
BMDMΦ IL-1α-/- + R. montanensis
F
C57BL/6 WT
IL-1β (pg/ml)
Day7
G
C57BL/6 WT
IL-1α (pg/ml)
Day7
H
Pathogenic Rickettsia
MΦ
Non-pathogenic Rickettsia
Phagolysosomal destruction
Ubiquitination
Endosome
Lysosome
Phagolysosomal destruction
Autophagy
pro-IL-1α
IL-1α
Caspase-11
GSDMD
Caspase-1
pro-IL-1β
IL-1β
MΦ
MΦ
Successful Host Colonization
Failed Host Colonization

Fig. 4

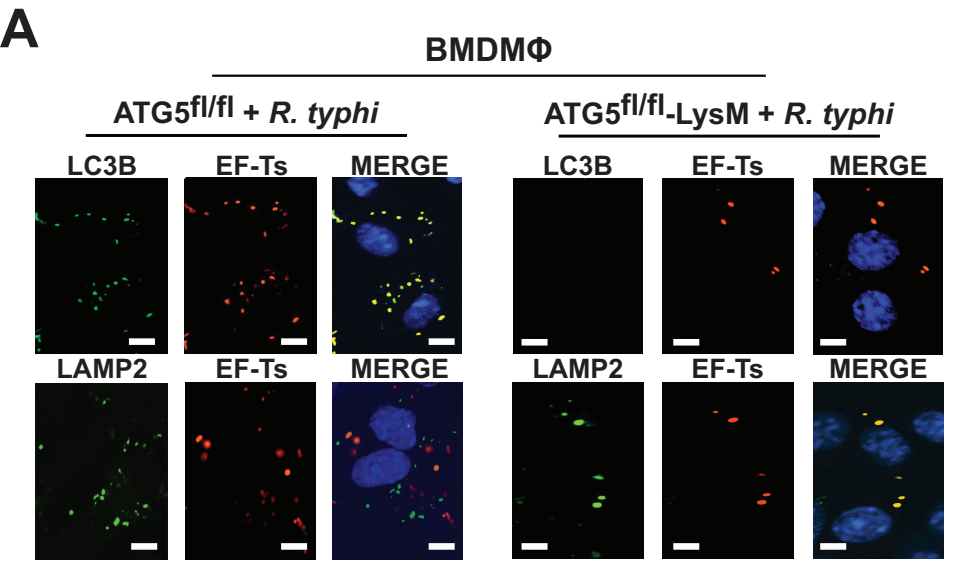
A
BMDMΦ
ATG5fl/fl + R. typhi
ATG5fl/fl-LysM + R. typhi
LC3B
EF-Ts
MERGE
LAMP2
EF-Ts
MERGE

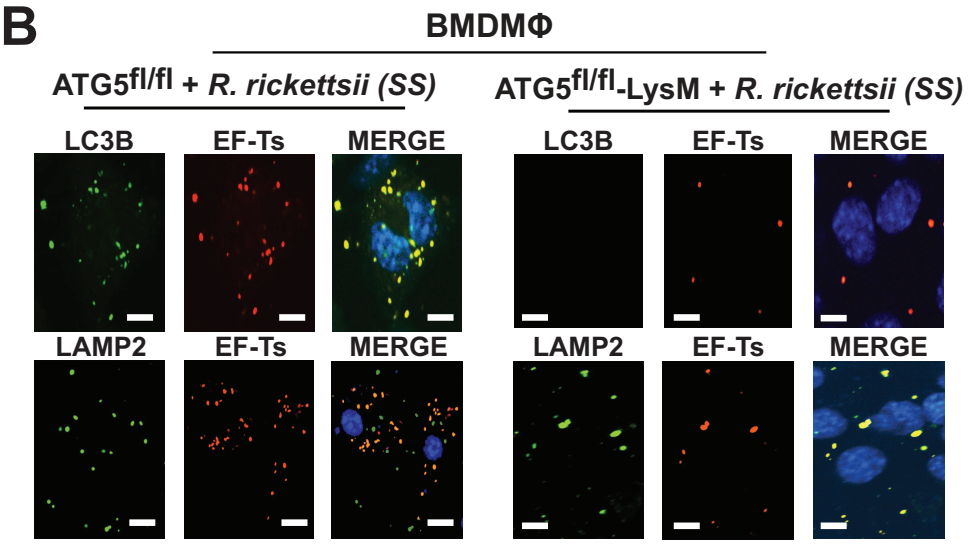
B
BMDMΦ
ATG5fl/fl + R. rickettsii (SS)
ATG5fl/fl-LysM + R. rickettsii (SS)
LC3B
EF-Ts
MERGE
LAMP2
EF-Ts
MERGE

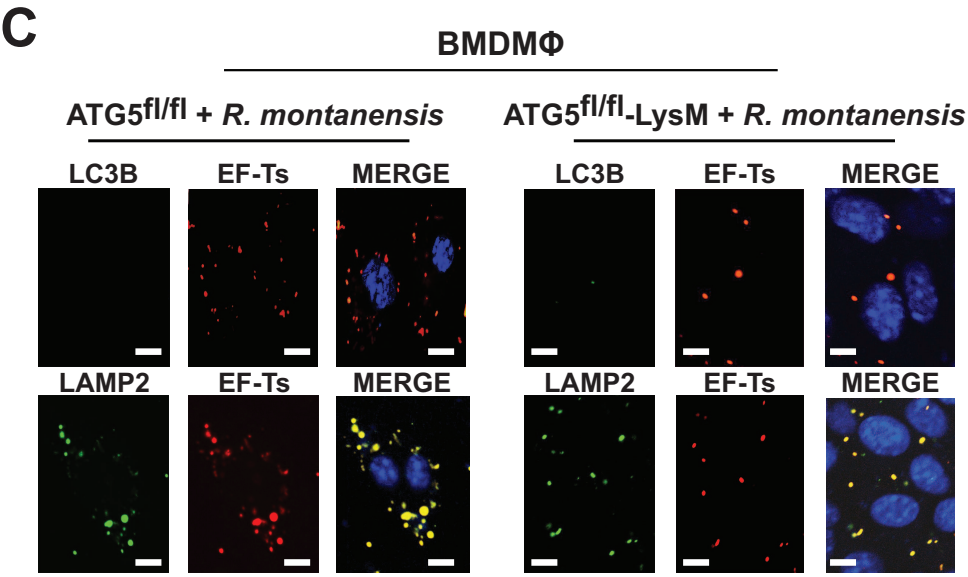
C
BMDMΦ
ATG5fl/fl + R. montanensis
ATG5fl/fl-LysM + R. montanensis
LC3B
EF-Ts
MERGE
LAMP2
EF-Ts
MERGE

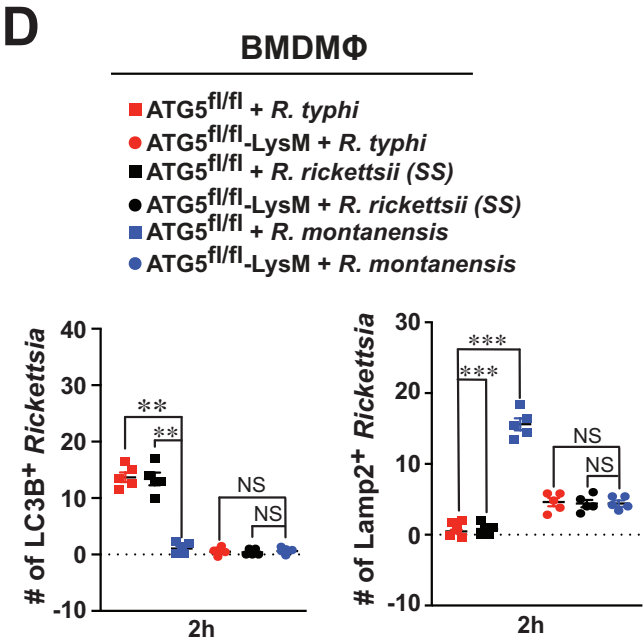
D
BMDMΦ
ATG5fl/fl + R. typhi
ATG5fl/fl-LysM + R. typhi
ATG5fl/fl + R. rickettsii (SS)
ATG5fl/fl-LysM + R. rickettsii (SS)
ATG5fl/fl + R. montanensis
ATG5fl/fl-LysM + R. montanensis
# of LC3B+ Rickettsia
# of Lamp2+ Rickettsia
2h
**
***
NS

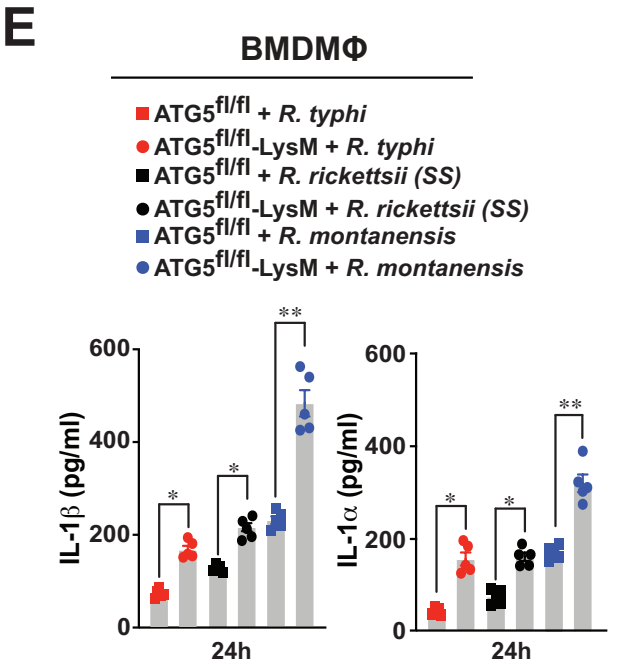
E
BMDMΦ
ATG5fl/fl + R. typhi
ATG5fl/fl-LysM + R. typhi
ATG5fl/fl + R. rickettsii (SS)
ATG5fl/fl-LysM + R. rickettsii (SS)
ATG5fl/fl + R. montanensis
ATG5fl/fl-LysM + R. montanensis
IL-1β (pg/ml)
IL-1α (pg/ml)
24h
*
**

Fig. S1

A

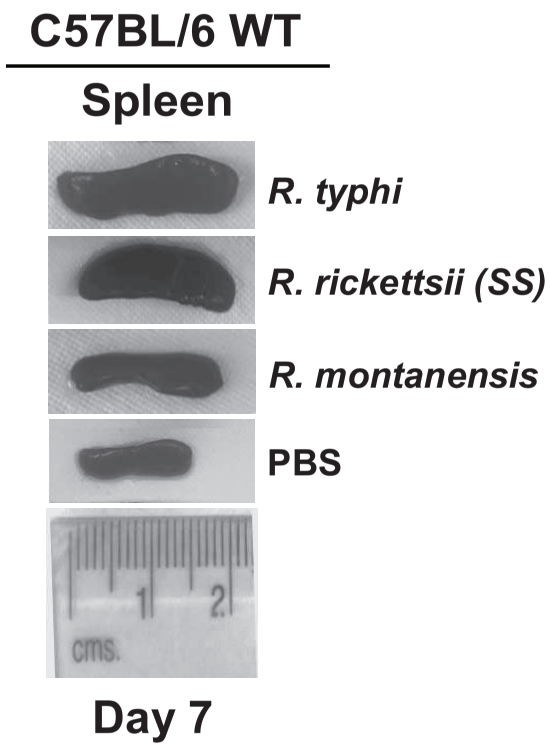
C57BL/6 WT
Spleen
R. typhi
R. rickettsii (SS)
R. montanensis
PBS
1
2
cms.
Day 7

B

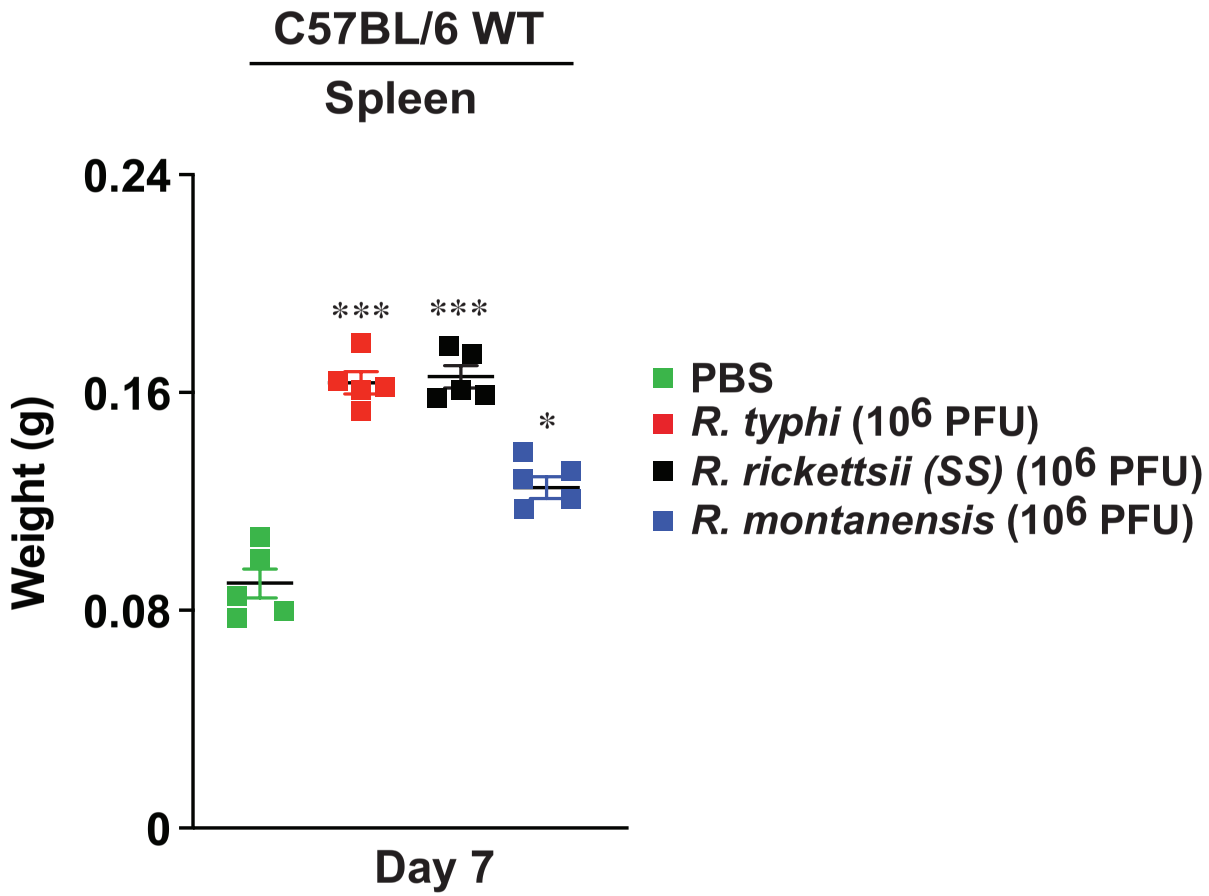
C57BL/6 WT
Spleen
0.24
0.16
0.08
0
Weight (g)
***
***
*
Day 7
PBS
R. typhi (10^6 PFU)
R. rickettsii (SS) (10^6 PFU)
R. montanensis (10^6 PFU)

Fig. S2

A

C57BL/6 WT

Spleen

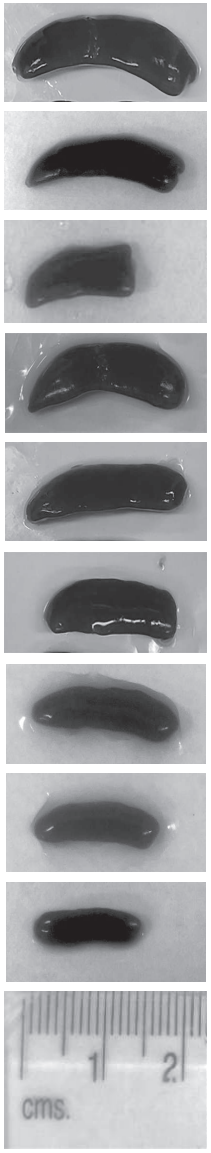

R. typhi + αIL-1α

R. typhi + αIL-1β

R. typhi + αIgG

R. rickettsii (SS) + αIL-1α

R. rickettsii (SS) + αIL-1β

R. rickettsii (SS) + αIgG

R. montanensis + αIL-1α

R. montanensis + αIL-1β

R. montanensis + αIgG

Day 7

B

C57BL/6 WT

Spleen

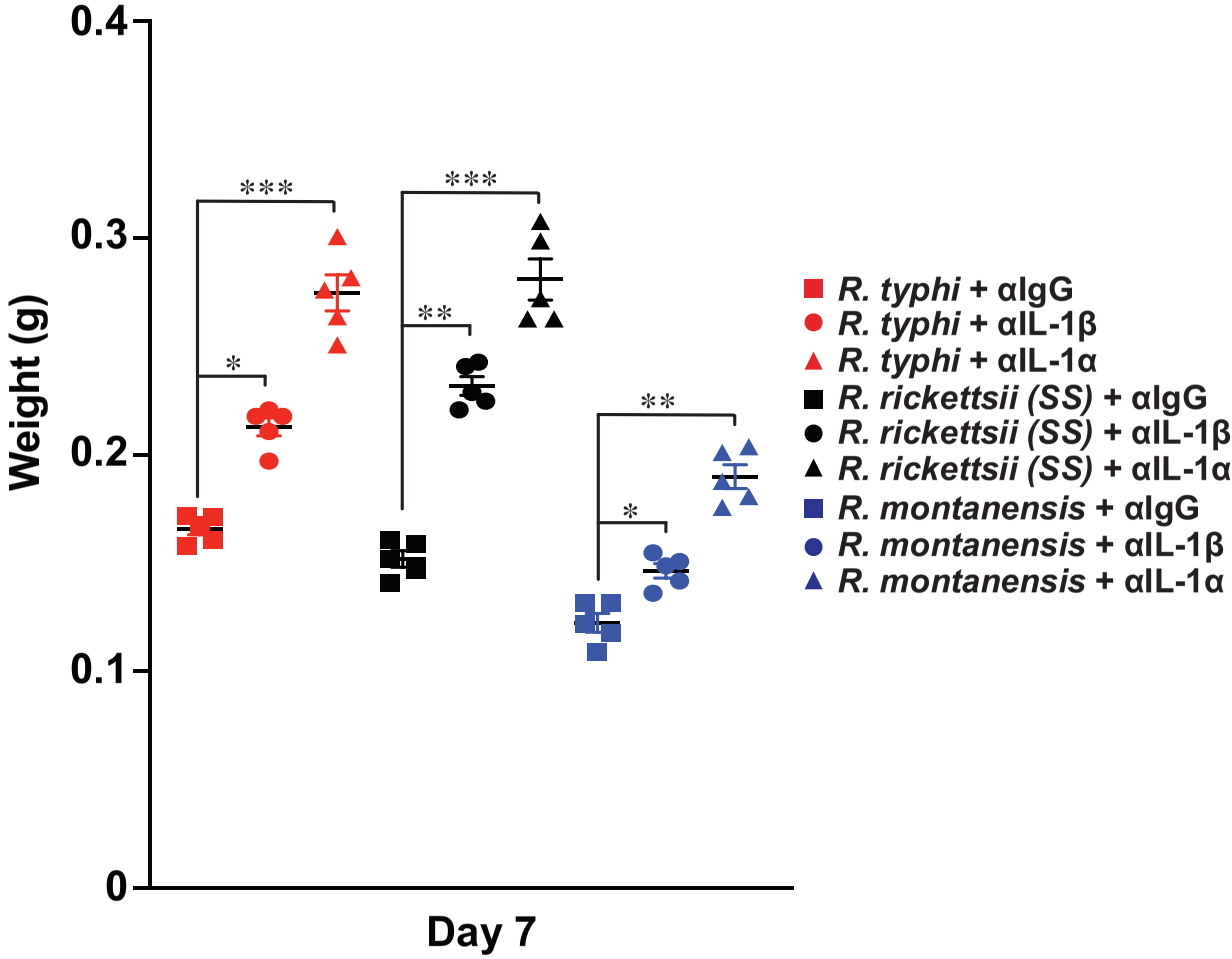

Fig. S3

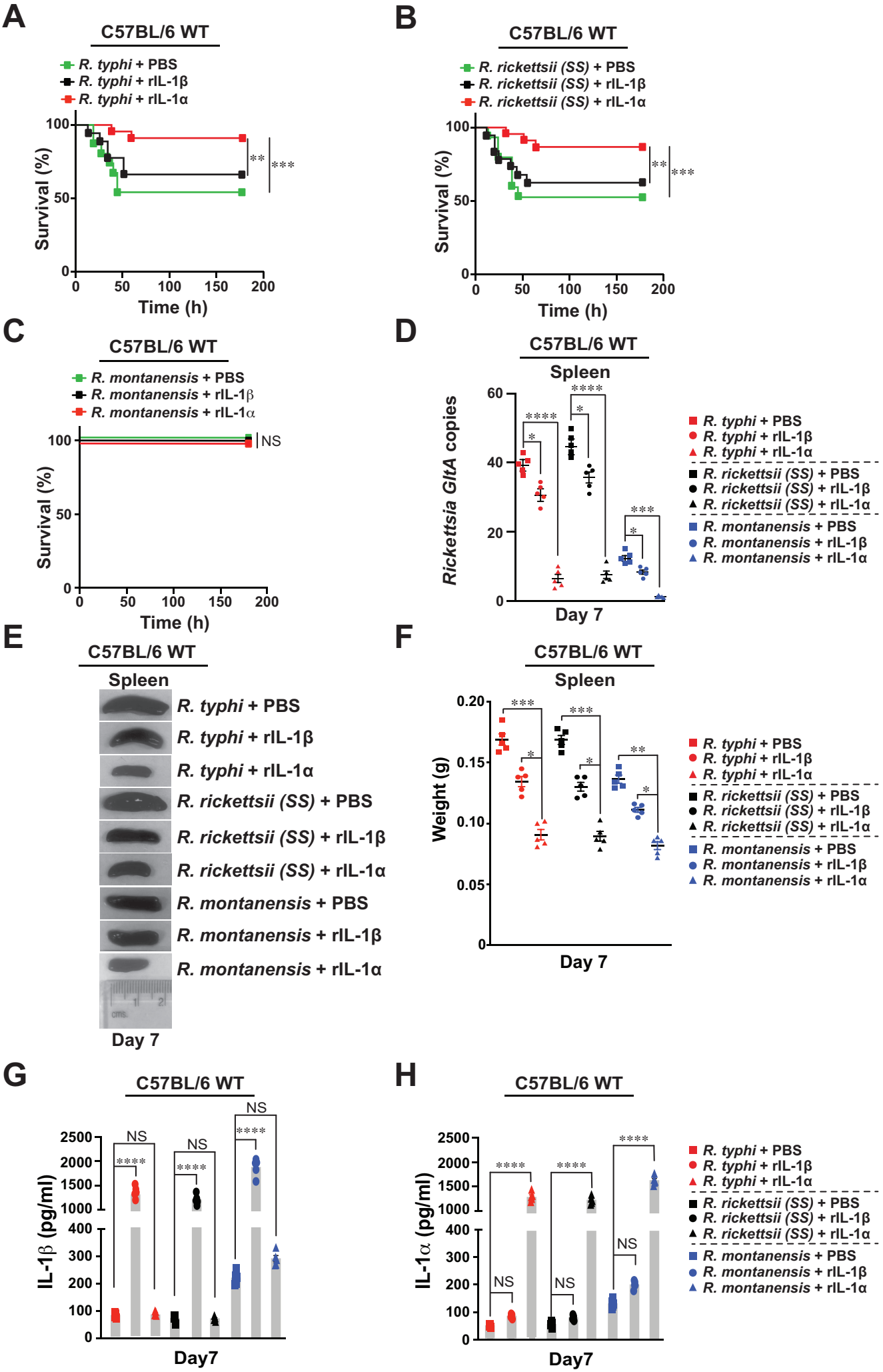
A
C57BL/6 WT
R. typhi + PBS
R. typhi + rIL-1β
R. typhi + rIL-1α
Survival (%)
Time (h)
B
C57BL/6 WT
R. rickettsii (SS) + PBS
R. rickettsii (SS) + rIL-1β
R. rickettsii (SS) + rIL-1α
Survival (%)
Time (h)
C
C57BL/6 WT
R. montanensis + PBS
R. montanensis + rIL-1β
R. montanensis + rIL-1α
NS
Survival (%)
Time (h)
D
C57BL/6 WT
Spleen
Rickettsia GltA copies
Day 7
R. typhi + PBS
R. typhi + rIL-1β
R. typhi + rIL-1α
R. rickettsii (SS) + PBS
R. rickettsii (SS) + rIL-1β
R. rickettsii (SS) + rIL-1α
R. montanensis + PBS
R. montanensis + rIL-1β
R. montanensis + rIL-1α
E
C57BL/6 WT
Spleen
R. typhi + PBS
R. typhi + rIL-1β
R. typhi + rIL-1α
R. rickettsii (SS) + PBS
R. rickettsii (SS) + rIL-1β
R. rickettsii (SS) + rIL-1α
R. montanensis + PBS
R. montanensis + rIL-1β
R. montanensis + rIL-1α
Day 7
F
C57BL/6 WT
Spleen
Weight (g)
Day 7
R. typhi + PBS
R. typhi + rIL-1β
R. typhi + rIL-1α
R. rickettsii (SS) + PBS
R. rickettsii (SS) + rIL-1β
R. rickettsii (SS) + rIL-1α
R. montanensis + PBS
R. montanensis + rIL-1β
R. montanensis + rIL-1α
G
C57BL/6 WT
IL-1β (pg/ml)
Day7
H
C57BL/6 WT
IL-1α (pg/ml)
Day7
R. typhi + PBS
R. typhi + rIL-1β
R. typhi + rIL-1α
R. rickettsii (SS) + PBS
R. rickettsii (SS) + rIL-1β
R. rickettsii (SS) + rIL-1α
R. montanensis + PBS
R. montanensis + rIL-1β
R. montanensis + rIL-1α

Fig. S4

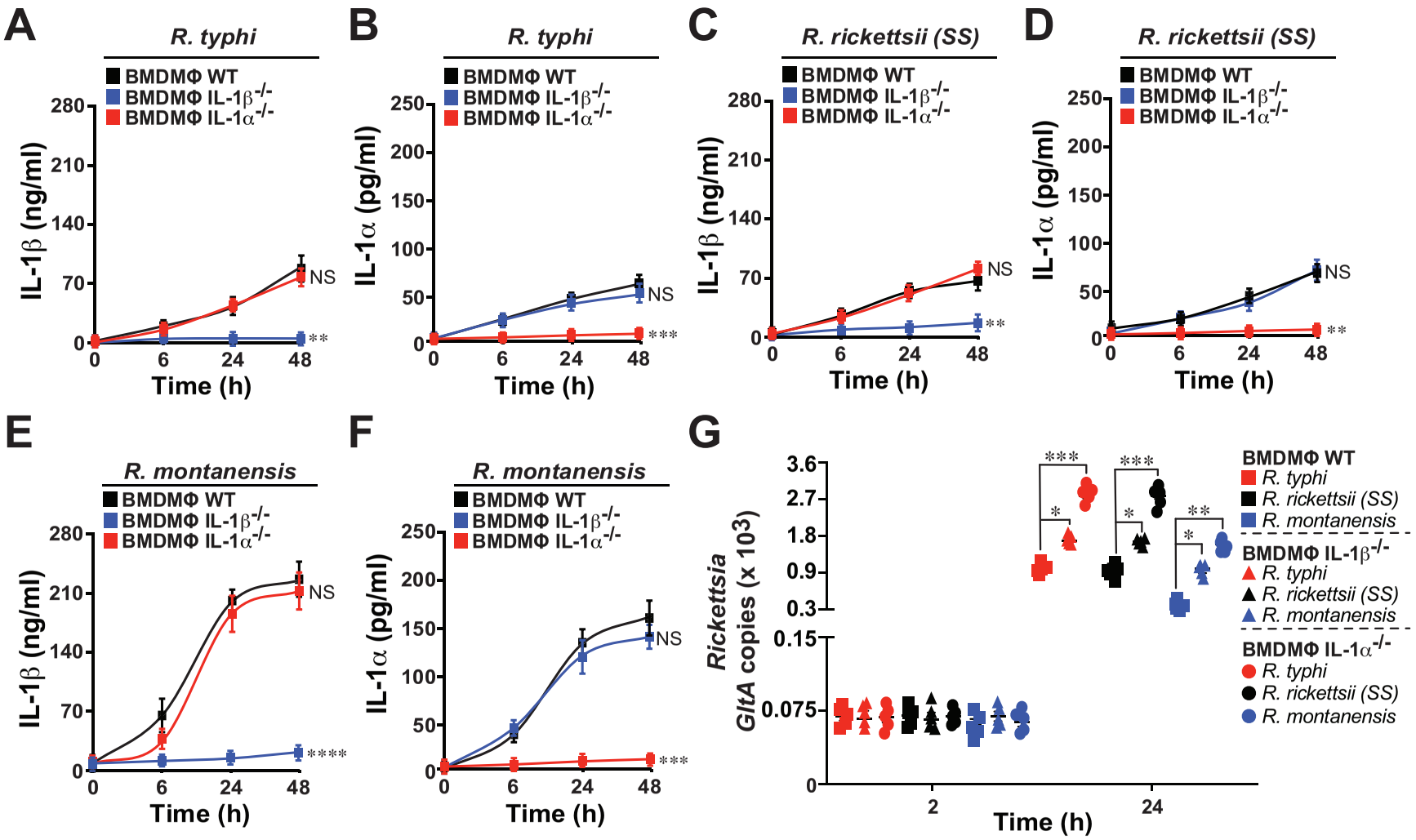
A
R. typhi
BMDMΦ WT
BMDMΦ IL-1β-/-
BMDMΦ IL-1α-/-
IL-1β (ng/ml)
Time (h)
NS
**
B
R. typhi
IL-1α (pg/ml)
NS
***
C
R. rickettsii (SS)
IL-1β (ng/ml)
NS
**
D
R. rickettsii (SS)
IL-1α (pg/ml)
NS
**
E
R. montanensis
IL-1β (ng/ml)
NS
****
F
R. montanensis
IL-1α (pg/ml)
NS
***
G
Rickettsia GltA copies (x 10^3)
Time (h)
BMDMΦ WT
R. typhi
R. rickettsii (SS)
R. montanensis
BMDMΦ IL-1β-/-
R. typhi
R. rickettsii (SS)
R. montanensis
BMDMΦ IL-1α-/-
R. typhi
R. rickettsii (SS)
R. montanensis

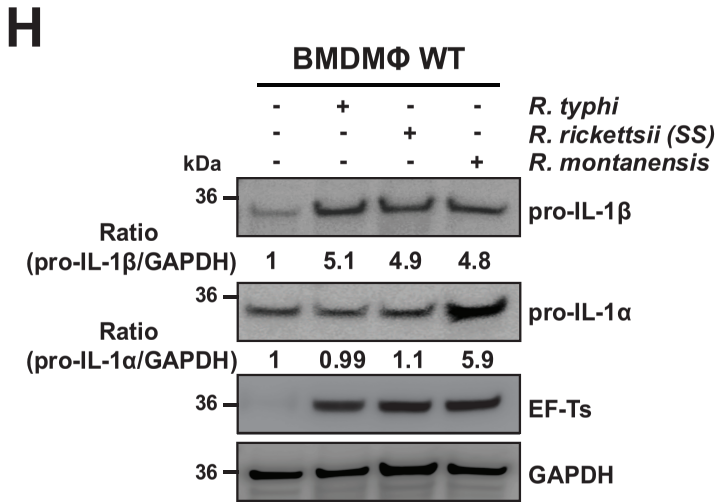
H
BMDMΦ WT
R. typhi
R. rickettsii (SS)
R. montanensis
kDa
36
pro-IL-1β
Ratio (pro-IL-1β/GAPDH) 1 5.1 4.9 4.8
pro-IL-1α
Ratio (pro-IL-1α/GAPDH) 1 0.99 1.1 5.9
EF-Ts
GAPDH

Fig. S5

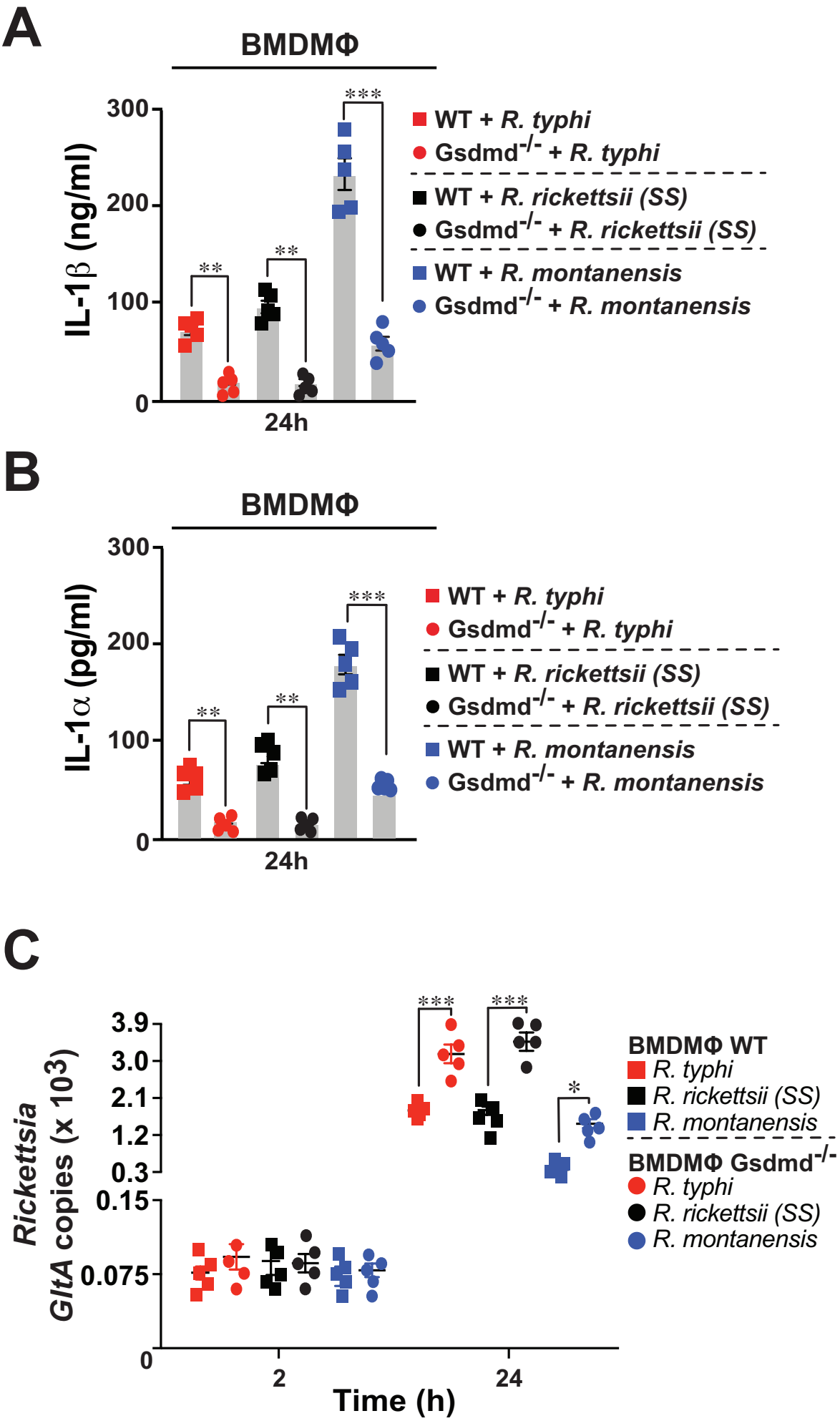
A
BMDMΦ
IL-1β (ng/ml)
300
200
100
0
24h
**
**
***
WT + R. typhi
Gsdmd-/- + R. typhi
WT + R. rickettsii (SS)
Gsdmd-/- + R. rickettsii (SS)
WT + R. montanensis
Gsdmd-/- + R. montanensis
B
BMDMΦ
IL-1α (pg/ml)
300
200
100
0
24h
**
**
***
WT + R. typhi
Gsdmd-/- + R. typhi
WT + R. rickettsii (SS)
Gsdmd-/- + R. rickettsii (SS)
WT + R. montanensis
Gsdmd-/- + R. montanensis
C
Rickettsia GltA copies (x 10^3)
3.9
3.0
2.1
1.2
0.3
0.15
0.075
0
2
24
Time (h)
***
***
*
BMDMΦ WT
R. typhi
R. rickettsii (SS)
R. montanensis
BMDMΦ Gsdmd-/-
R. typhi
R. rickettsii (SS)
R. montanensis

Fig. S6

A

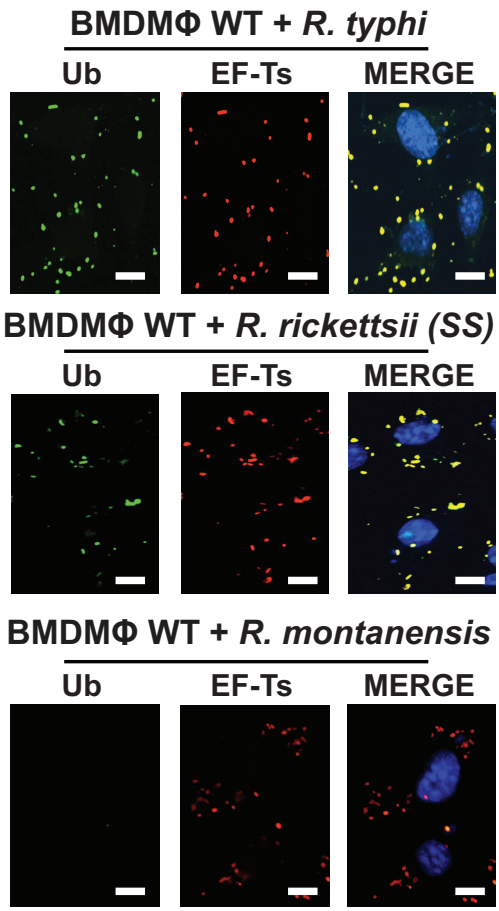
BMDMΦ WT + R. typhi
Ub
EF-Ts
MERGE
BMDMΦ WT + R. rickettsii (SS)
Ub
EF-Ts
MERGE
BMDMΦ WT + R. montanensis
Ub
EF-Ts
MERGE

B

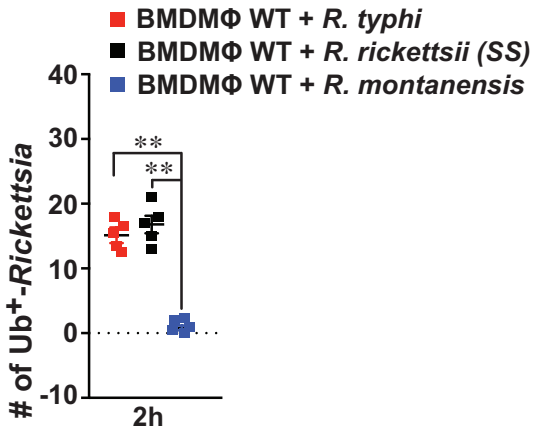
BMDMΦ WT + R. typhi
BMDMΦ WT + R. rickettsii (SS)
BMDMΦ WT + R. montanensis
# of Ub+-Rickettsia
40
30
20
10
0
-10
**
**
2h

C

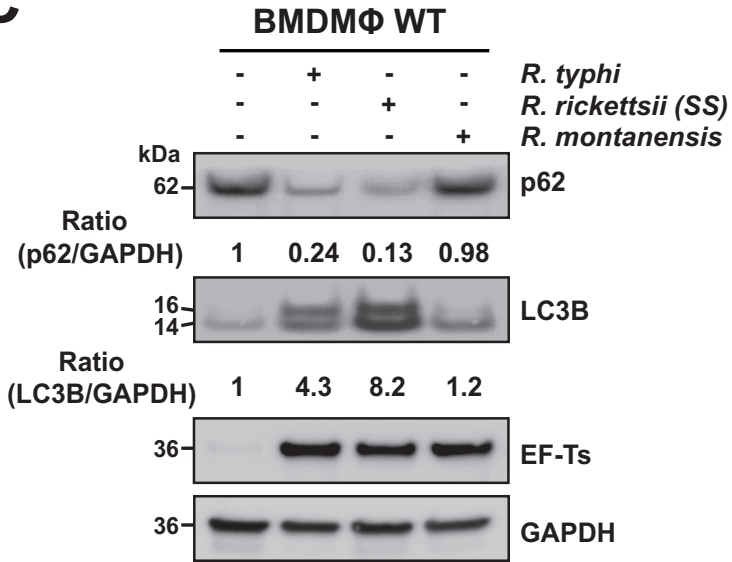
BMDMΦ WT
- + - - R. typhi
- - + - R. rickettsii (SS)
- - - + R. montanensis
kDa
62
p62
Ratio (p62/GAPDH) 1 0.24 0.13 0.98
16
14
LC3B
Ratio (LC3B/GAPDH) 1 4.3 8.2 1.2
36
EF-Ts
36
GAPDH

Fig. S7

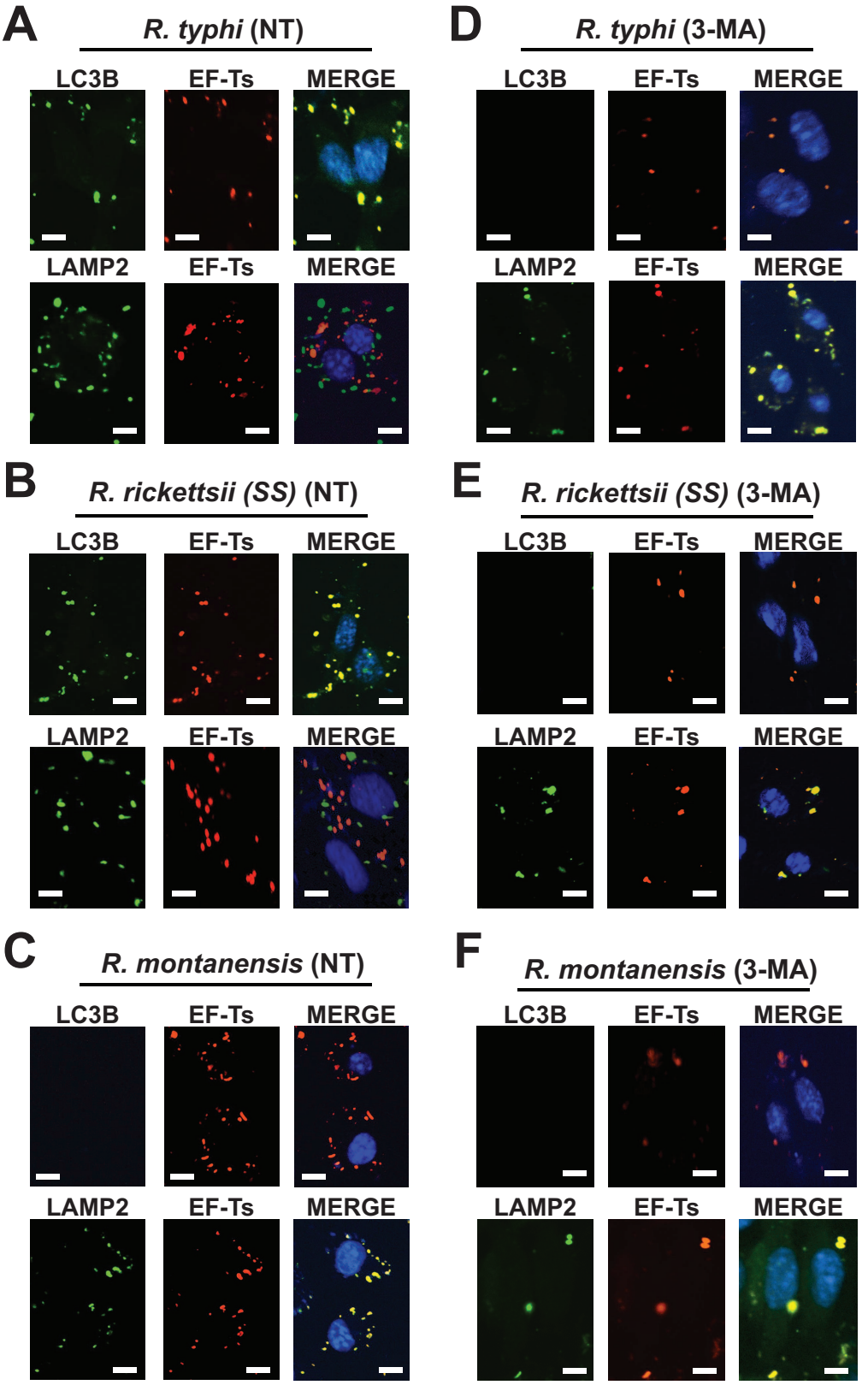
A
R. typhi (NT)
LC3B
EF-Ts
MERGE
LAMP2
EF-Ts
MERGE
D
R. typhi (3-MA)
LC3B
EF-Ts
MERGE
LAMP2
EF-Ts
MERGE
B
R. rickettsii (SS) (NT)
LC3B
EF-Ts
MERGE
LAMP2
EF-Ts
MERGE
E
R. rickettsii (SS) (3-MA)
LC3B
EF-Ts
MERGE
LAMP2
EF-Ts
MERGE
C
R. montanensis (NT)
LC3B
EF-Ts
MERGE
LAMP2
EF-Ts
MERGE
F
R. montanensis (3-MA)
LC3B
EF-Ts
MERGE
LAMP2
EF-Ts
MERGE

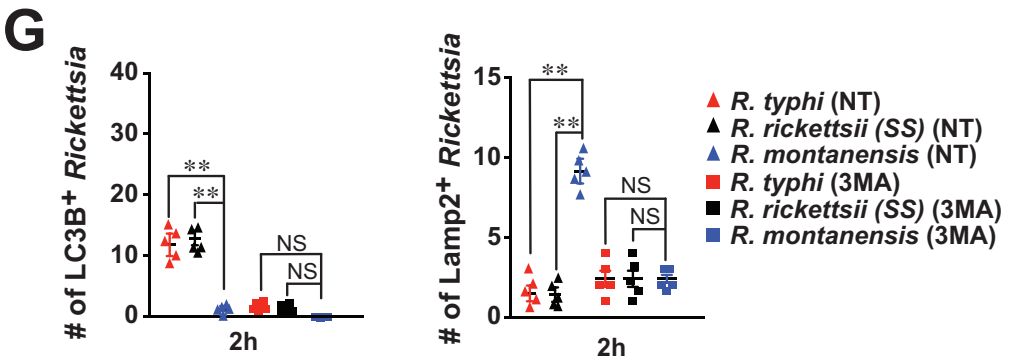
G
# of LC3B+ Rickettsia
40
30
20
10
0
**
**
NS
NS
2h
# of Lamp2+ Rickettsia
15
10
5
0
**
**
NS
NS
2h
R. typhi (NT)
R. rickettsii (SS) (NT)
R. montanensis (NT)
R. typhi (3MA)
R. rickettsii (SS) (3MA)
R. montanensis (3MA)

Fig. S8

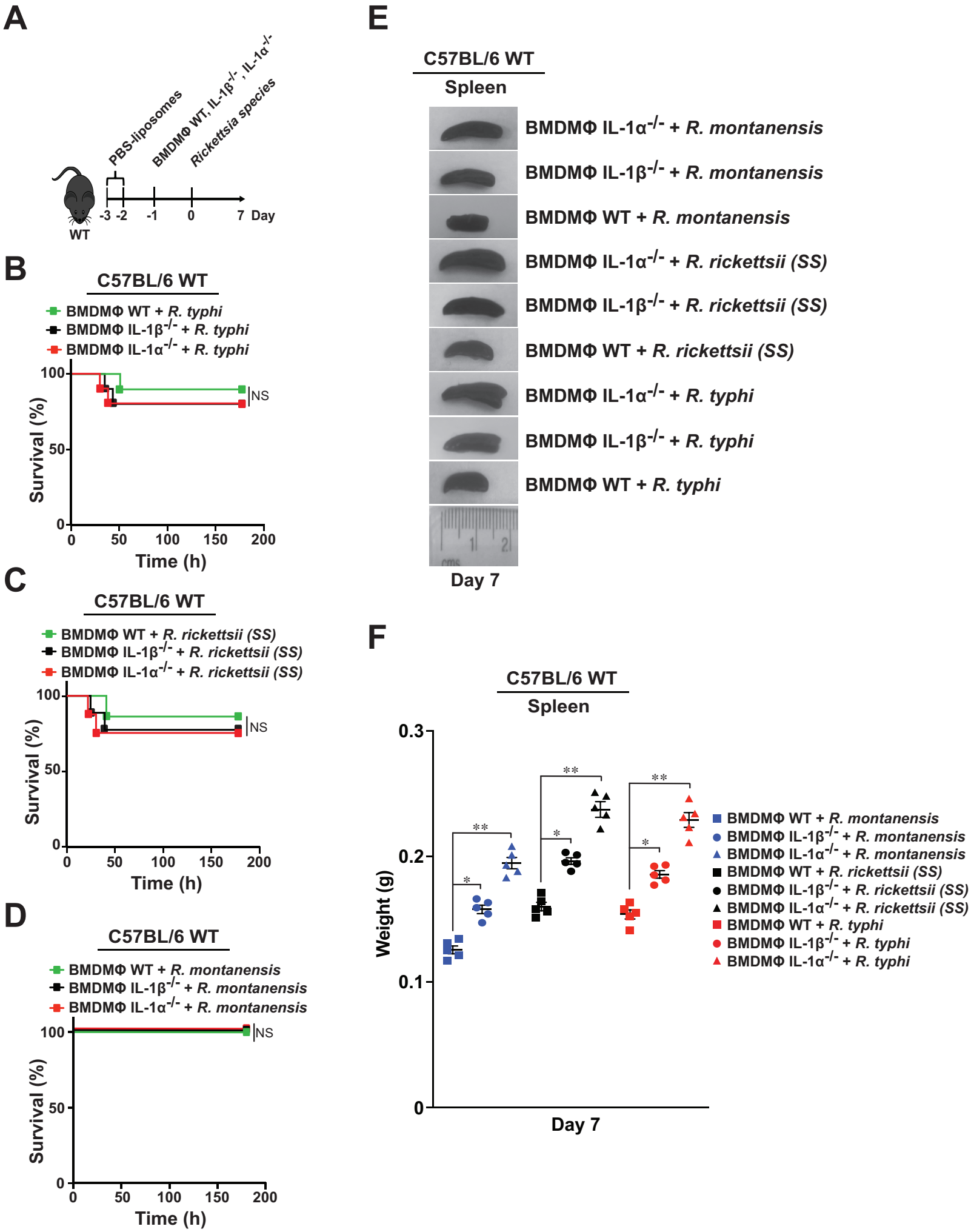
A
PBS-liposomes
BMDMΦ WT, IL-1β-/-, IL-1α-/-
Rickettsia species
-3 -2 -1 0 7 Day
WT
B
C57BL/6 WT
BMDMΦ WT + R. typhi
BMDMΦ IL-1β-/- + R. typhi
BMDMΦ IL-1α-/- + R. typhi
Survival (%)
Time (h)
NS
C
C57BL/6 WT
BMDMΦ WT + R. rickettsii (SS)
BMDMΦ IL-1β-/- + R. rickettsii (SS)
BMDMΦ IL-1α-/- + R. rickettsii (SS)
Survival (%)
Time (h)
NS
D
C57BL/6 WT
BMDMΦ WT + R. montanensis
BMDMΦ IL-1β-/- + R. montanensis
BMDMΦ IL-1α-/- + R. montanensis
Survival (%)
Time (h)
NS
E
C57BL/6 WT
Spleen
BMDMΦ IL-1α-/- + R. montanensis
BMDMΦ IL-1β-/- + R. montanensis
BMDMΦ WT + R. montanensis
BMDMΦ IL-1α-/- + R. rickettsii (SS)
BMDMΦ IL-1β-/- + R. rickettsii (SS)
BMDMΦ WT + R. rickettsii (SS)
BMDMΦ IL-1α-/- + R. typhi
BMDMΦ IL-1β-/- + R. typhi
BMDMΦ WT + R. typhi
Day 7
F
C57BL/6 WT
Spleen
Weight (g)
Day 7
BMDMΦ WT + R. montanensis
BMDMΦ IL-1β-/- + R. montanensis
BMDMΦ IL-1α-/- + R. montanensis
BMDMΦ WT + R. rickettsii (SS)
BMDMΦ IL-1β-/- + R. rickettsii (SS)
BMDMΦ IL-1α-/- + R. rickettsii (SS)
BMDMΦ WT + R. typhi
BMDMΦ IL-1β-/- + R. typhi
BMDMΦ IL-1α-/- + R. typhi